Journal Pre-proof

Indole chalcones: Design, synthesis, *in vitro* and *in silico* evaluation against *Mycobacterium tuberculosis*

Deepthi Ramesh, Annu Joji, Balaji Gowrivel Vijayakumar, Aiswarya Sethumadhavan, Maheswaran Mani, Tharanikkarasu Kannan

PII: S0223-5234(20)30328-7

DOI: https://doi.org/10.1016/j.ejmech.2020.112358

Reference: EJMECH 112358

To appear in: *European Journal of Medicinal Chemistry*

Received Date: 10 March 2020

Revised Date: 4 April 2020

Accepted Date: 16 April 2020

Please cite this article as: D. Ramesh, A. Joji, B.G. Vijayakumar, A. Sethumadhavan, M. Mani, T. Kannan, Indole chalcones: Design, synthesis, *in vitro* and *in silico* evaluation against *Mycobacterium tuberculosis*, *European Journal of Medicinal Chemistry* (2020), doi: https://doi.org/10.1016/j.ejmech.2020.112358.

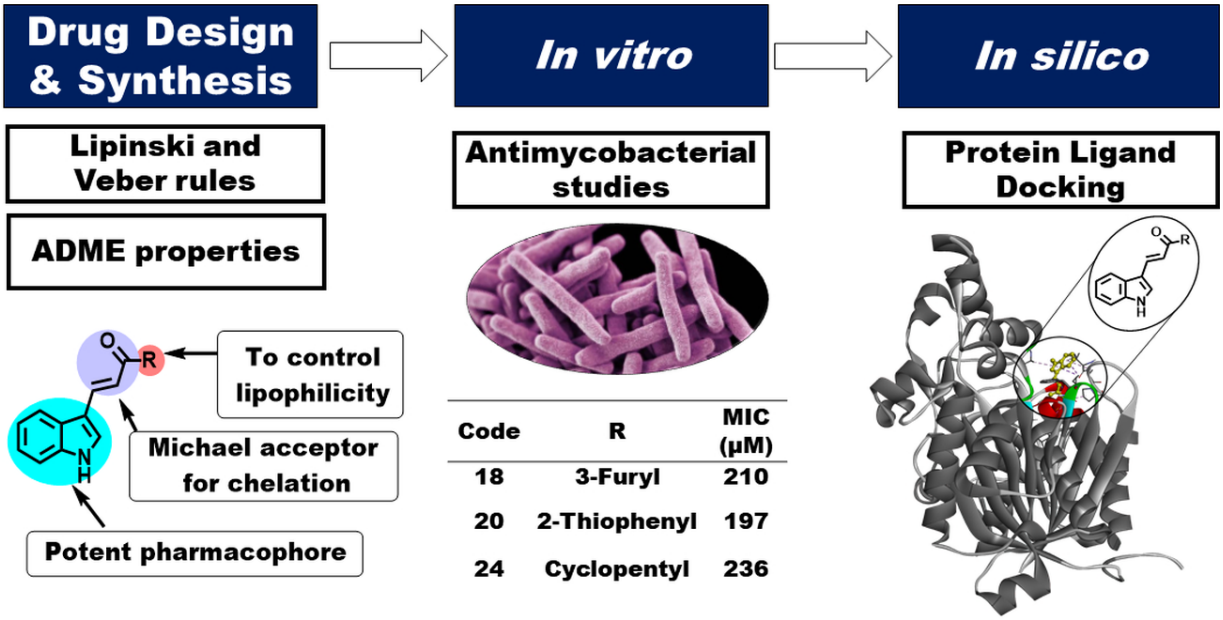

Indole chalcones: Design, Synthesis, *in vitro* and *in silico* evaluation against *Mycobacterium tuberculosis*

Deepthi Ramesh[a], Annu Joji[a], Balaji Gowrivel Vijayakumar[a], Aiswarya Sethumadhavan[b], Maheswaran Mani[b], Tharanikkarasu Kannan[a,*]

[a] Department of Chemistry, Pondicherry University, Kalapet, Puducherry-605014, India.

[b] Department of Microbiology, Pondicherry University, Kalapet, Puducherry-605014, India.

Corresponding author: Tel: +91-413-265 4411; Fax: +91-413-265 6740.

Email address: tharani.che@pondiuni.edu.in

Abstract

Indole chalcones were designed and synthesized as a promising set of compounds against H_{37}Rv strain of *Mycobacterium tuberculosis*. Within this library of compounds, (*E*)-1-(furan-3-yl)-3-(1*H*-indol-3-yl)prop-2-en-1-one (**18**), (*E*)-3-(1*H*-indol-3-yl)-1-(thiophen-2-yl)prop-2-en-1-one **(20)** and (*E*)-2-((1*H*-indol-2-yl)methylene)cyclopentan-1-one (**24**) displayed high anti-tubercular activity at 50 µg/ml with MIC values of 210, 197 and 236 µM respectively. The *in-silico* studies revealed that compound **18** exhibit binding modes similar to FAS-II inhibitors like INH or Thiolactomycin against KasA protein. Cytotoxicity assay results suggest that the compounds **18**, **20** and **24** are non-cytotoxic to human megakaryocytes and murine B cells.

Keywords: Indole chalcones, Anti-tubercular, *Mycobacterium tuberculosis*, H_{37}Rv strain, Luciferase reporter mycobacteriophages (LRP), SARs, KasA protein, Cytotoxicity

1. Introduction

Tuberculosis (Tb) is an airborne communicable ailment with high fatality rates ranking above HIV/AIDS [1]. Out of 10 million new Tb infected people in 2018, there were approximately 1.5 million deaths [1]. Though Tb became epidemic during the industrial revolution, it was brought under control with the launch of BCG (Bacillus Calmette–Guérin) vaccine in 1921 followed by antibiotics such as streptomycin (1943), isoniazid (1952) and rifampicin (1963). Tb incidence also increased with HIV infection during the 1980s, and out of 10 million Tb deaths in 2018, 2,51,000 people were HIV positive [1]. To combat this disease, presently four orally active antimicrobial agents such as isoniazid (INH), pyrazinamide (PZA), rifampicin (RIF) and ethambutol (EMB) are administered for two months succeeded by INH RIF combination over a span of 4 months [2]. Even with all these efforts [3], Tb is widespread and with emerging drug-resistance such as multi-drug-resistant Tb (MDR-Tb), extensively-drug-resistant Tb (XDR-Tb) and totally-drug-resistant Tb (TDR-Tb) strains, this disease increasingly hard to eradicate. The disease complexity, long period of the treatment, practicality of drug sensitivity tests and lack of proper diagnosis are considerable challenges. In addition to this, drugs such as INH and RIF show severe side effects such as hepatotoxicity. To overcome these issues, several strategies like repurposing and revival of drugs such as Clofazimine [4], structure and mechanism based drug design which involves genome sequencing and identification of molecular targets [5], molecular hybridisation of active pharmacophores [6] have been explored to find an ideal drug. An ideal Tb drug should fulfil the criteria of improving the treatment of latent Tb, have zero interactions with HIV medicines, lower dosage with improved efficacy, enhanced bioavailability and target both MDR and XDR Tb strains [7]. A wide range of compounds have been screened to find a novel ideal drug for curing Tb [2, 8]. In Tb drug discovery research, there are four promising types of targets.

Tetrahydropyrans [9], diarylethers [10], methylthiazole [2], aminoproline [11], aryl amides [12], piperazine indoleformamides [13], imidazopiperidines [14] etc. were used for targeting Fatty acid synthase II (FASII) enoylacyl carrier protein reductase (InhA). Adamantyl ureas [15], phenyl pyrroles [16], benzimidazoles [2], indolecarboxamides [17] etc. were used for targeting Transmembrane transport protein large (MmpL3). Benzothiazinone [18], benzothiazoles [19], 1,4-azaindoles [20], 4-aminoquinolone piperidine amides [21] etc. were used for targeting Decaprenylphospho-beta-D-ribofuranose and phthalimide and quinoline containing compounds were used for targeting 2-oxidase (DprE1) [2].

Most of these compounds as well as commercial drugs have N-containing heterocyclic moieties and they are one of the most sought-after pharmacophores for designing new and efficient drugs in the pharmaceutical industry. Indole heterocycle is an important bioactive compound and it serves as a crucial skeleton in naturally occurring alkaloids like tryptophan (an amino acid), serotonin (a naturally-occurring neurotransmitter in humans), reserpine (a tranquillizer isolated from the plant *Rauvolfia serpentina*), and indole 3-acetic acid (a phytohormone) [22]. In addition, marine and bacterial indole alkaloids show anti-cancer [23], anti-viral [24] , anti-bacterial [25], and anti-HIV [26] properties. Moreover, indole derivatives are known for their role as antimicrobial [27, 28], antiviral [29], insecticidal [30], painkillers [31], anti-inflammatory [32], depression medications [33], anti-tubercular [20, 34], antineoplastic [35], antihypertensives [36], antioxidants [23], and anti-diabetic [33] agents. The Food and Drug Administration (FDA) has even published a database highlighting the importance of N-containing heterocyclic compounds in 2015 and indole derivatives ranks 9th among the top 25 FDA approved drugs with 17 indole containing drugs in the market [37]. There are two active indole-based lead candidates, NITD-304 and NITD-349 (recognised as MmpL3 inhibitors: see **Fig. 1(a)** for structure) which are in the clinical stage of evaluation for drug-sensitive Tb strains [38]. MmpL3 is a transporter from Mycobacterial Membrane Protein Large (MmpL) and carries mycolic acids as trehalose monomycolates (TMM) across the cell

membrane for biosynthesis of Tb cell wall [39]. MmpL3 is a strategic drug target for MDR and XDR Tb strains where treatment and survival options are limited. Similar to indole derivatives, chalcones are also important pharmacophores which are (1,3-diarylprop-2-en-1-one) flavonoids found in a number of natural products [40]. They impart strong colouration to plant pigments and occur in many plant species such as *Glycyrrhiza inflate* [41], *Angelica keiskei* [42], and *Piper aduncum* [43]. Chalcones can exist in *E* and *Z* forms with *E* isomer being more stable [40] and showed antioxidant [44], anti-HIV [45], anti-alzheimer's disease [46-48], antibacterial [49], antileishmanial [48, 50], anticancer [51], antimalarial [52, 53], antiviral [48] and antitubercular [48, 52] properties. The alkene bond fused with carbonyl group is accountable for the bioactivity of chalcones, though the exact mechanism of activity is still under investigation [40, 54]. Chalcones have inhibitory effects on various enzymes like trypsin and topoisomerases due to complex formation of chalcone with the active sites of the enzymes [55].

Considering the above aspects and in a quest to find novel anti-Tb agents, molecular hybridisation in drug designing is considered in the present investigation by hybridising indole and chalcone. Hybrid molecules can have modified selectivity, contrasting approaches of action, lesser unwanted aftereffects, improved solubility and oral bioavailability [56, 57]. There has been limited exploration of chalcones as antitubercular agents and indole chalcones, in general, are not well reported. There are few reports of indole chalcones showing biological activity [58-60] as shown in **Fig. 1b**. Till date, as per our knowledge, there are no reports on using indole chalcones as antitubercular agents. Hence, in our endeavour to synthesize novel antitubercular agents [61, 62], we have designed and synthesized indole-chalcone hybrids with aromatic, heteroaromatic and fused rings. The basicity of the compounds was taken into consideration for improved cell permeability. The compounds are analysed *in vitro* with $H_{37}Rv$ strain of *Mycobacterium tuberculosis* (*MTb*) to discover their promising mycobacterial properties and the results are presented in this paper.

< Insert Fig. 1>

2. Experimental section

2.1. Materials and Methods

Indole-3-carboxaldehyde was bought from Avra Synthesis, Hyderabad, India. Acetophenones and piperidine were procured from Avra Synthesis, Hyderabad, India and Sigma-Aldrich, USA. Absolute ethanol from Spectrochem Pvt. Ltd, Mumbai, India was used directly. Nuclear Magnetic Resonance spectra (NMR) were recorded in 400 MHz for ^{1}H NMR and 101 MHz for ^{13}C NMR on a Bruker Avance-400 spectrometer. The internal reference compound used was trimethylsilane. Mass spectra were acquired using AGILENT Technologies 6530B Accurate Mass QTOF-LC/MS. Thermo Nicolet 6700 spectrometer recorded Fourier transform infrared spectra (FT-IR). Single crystal X-ray diffraction data were acquired by Xcalibur Eos, Rigaku Oxford Diffraction instrument X-ray diffractometer of Mo-Kα radiation (λ = 0.71073 Å). Empirical absorption was done using SCALE3 ABSPACK scaling algorithm. The refinement was carried out by XL, in the Olex 2-1.2 package plus structural solution by SHELXS-97. For cytotoxicity, the human megakaryocyte cell line Mo7e (ACC 104) and Murine pro B cell line BA/F3 (ACC 300) were attained from German Collection of Microorganisms and Animal Cell Cultures, DSMZ, Germany. Mo7e and BA/F3 cells were maintained in RPMI 1640 medium (Gibco, Waltham, MA USA) with 10 % fetal calf serum (HiMedia, India) in the presence of 20 ng/ml human IL-3 and murine IL-3 (Peprotech Asia, Rehovot, Israel) respectively.

2.2. *Synthesis of indole chalcone derivatives*

In an RB flask, 1H-indole-3-carboxaldehyde (1 mmol) and appropriate acetophenones (1.2 mmol) were taken and 5 ml of ethanol and 5 drops of piperidine were added. The resulting solution was then refluxed at 70°C and TLC was used to track the reaction process. Upon accomplishement of the reaction, the reaction mixture was transferred into cold water and further neutralized utilizing 1N hydrochloric acid. The crude precipitate formed was filtered out, dried and recrystallized from chloroform. All the indole chalcones (**1** to **25**) were characterized using spectral techniques and the spectral data are listed in the supplementary data.

2.3. *In vitro anti-Tb activity studies*

2.3.1. *Preparation of sample*

The initial stock solution was made by the dissolution of 10mg of a sample in 1mL of DMSO. The working stock solutions of 1 mg/mL and 0.5 mg/mL were prepared from this stock solution by adding the required volume of Middlebrook 7H9 broth and further sterilized by filtration using 0.45 µ filter.

2.3.2. *Luciferase reporter mycobacteriophages (LRP) assay*

Four cryovials per set (two for control and two for 100 µg/mL and 50 µg/mL concentrations) were taken. 400 µl of Middlebrook 7H9 broth was transferred into first two vials and 350 µl in the third and fourth vial. About 50 µl of 1mg/mL of stock was added to the 3rd and 4th vial respectively to get a total concentration of 400 µl. 100 µl of *M.Tb* H_{37}Rv cell

suspension was further introduced to the vials and incubated the vials at 37 °C for 72 h. Then, 50 µl of phage phAE202 and 40 µl of 0.1M $CaCl_2$ were introduced to all the vials (cell-phage mixture) and incubated at 37 °C for 4 h. Post incubation, 100 µl of the cell-phage mixture was moved to a luminometer cuvette. 100 µl of D-luciferin was introduced and thereafter the relative light unit (RLU) was determined instantly in a luminometer (Berthold) at 10S integration. The percentage of reduction in RLU of the test compared to control was calculated by using the following equation,

$$Percentage\ of\ Reduction\ in\ RLU = \frac{Control\ RLU - Test\ RLU}{Control\ RLU} \times 100$$

Compounds with RLU reduction of 50% and above in comparison with control were considered as active against *MTb*.

2.4. *Molecular Docking*

Docking was executed using AutoDock Vina v.1.1.2 [63] at maximum exhaustiveness of 8 for the blind protein-ligand docking. The crystal data of Tb proteins (PDB IDs: 2WGD, 6AJH, 3IFZ, 4B6C, 1ZID, 4FDO, 1N40) from the RCSB Protein Data Bank (PDB) were used. The structure was handpicked based on the highest resolution and lowest R factors. Using AutoDock Tools v.1.5.6., extraneous solvent molecules and co-crystallized ligands were removed from the protein. Only polar hydrogens were taken into account and gaussian and gasteiger charges were assigned as preparation for docking. Energy minimized ligand files were prepared using Perkin-Elmer Chem3D v15.0. Automation of the docking process was done with the use of PyRx-Python Prescription v0.8 [64]. Binding affinity values in kcal mol^{-1} were noted provided that root means square deviation (RMSD) values were below 2Å. Analysis

of binding mode of the selected drug candidates post-docking was performed on BIOVIA Discovery Studio Visualizer v.19.1.0 [65] to visualize the protein-ligand interactions.

2.5. Cytotoxicity assay

Cell cytotoxicity assay was carried out using WST-1 (Roche, Basel, Switzerland) by considering the manufacturer's protocol. Mo7e and BA/F3 cells were plated in 96-well tissue culture plate at a concentration of 20,000 cells per well in 100 µL of media. It was stimulated with different concentrations of compounds 18, 20 and 24 for 24 h. Cells were also treated only with DMSO to exclude solvent-induced cytotoxicity and 10 µL of WST-1 reagent was added after incubation. The absorbance was measured against a background control as blank using microplate (ELISA) reader at 440 nm. Statistical analysis was done using Graphpad Prism v.6.0.1 (GraphPad Software, Inc., CA, US) and P value of <0.05 were deemed substantial.

3. Results and Discussion

In a constant attempt to identify potential candidates against the virulent *MTb*, novel 2-aminothiazole derivatives have been successfully synthesized in our lab and reported by our research group [61, 62]. In continuation of this effort, in the extant research, a library of novel indole-chalcones was designed, synthesized and screened against $H_{37}Rv$ strain of *MTb*. Furthermore, *in-silico* anti-Tb activities against KasA protein present in *MTb* were carried out. In our survey of existing literature, till date, indole chalcones have not been reported as active compounds against Tb. Here, indole chalcone derivatives have been designed with hydrophilic and lipophilic properties, and the indole core is retained in all the compounds as the active

pharmacophoric fragment. The chalcone unit acts as the Michael acceptor and various groups have been introduced in this unit for cell permeability and solubility.

3.1. Design of indole chalcone derivatives

The pharmacokinetic properties of a drug should be known before synthesizing the drug for better biological action. Hence, the indole chalcone compounds were designed using the Lipinski [66] and Veber rules [67] for drug-likeness. Indole scaffold was retained in all the compounds and substituted, fused, heteroaromatic rings were incorporated to induce lipophilicity of indole chalcone derivatives. Additionally, aliphatic rings were also incorporated for this purpose. It is widely accepted that by inducing lipophilicity, permeation of any drug into the cell wall of Tb can be achieved. **Table 1** shows the list of indole chalcones designed for the present investigation. Molinspiration server [68] was used to gather the pharmacokinetic properties of the indole chalcones and the properties are compiled in **Table 2**. According to the data, the molar mass of the indole chalcones is less than 500 ranging from 211.26-347.42 which indicates that they can be easily metabolised in comparison to larger molecules. The Log P suggests the lipophilicity and values for indole chalcones are in the range of 2.49- 5.07. Log P value of indole chalcones are in the recommended range, except for compound **5** which has higher Log P values of 5.07. Interestingly, all the compounds possess 1-3 H-bond donors and 2-5 H-bond acceptors. Out of 25 compounds designed, 24 are found to obey Lipinski Rule and found to have drug-like character. Other parameters like topological polar surface area (TPSA) and a sum of rotatable bonds were also evaluated. TPSA is associated with the hydrogen bonding of the molecule and bioavailability of a drug. TPSA values are in the range of 32.86 to 78.69 and the count of rotatable bonds in the range of 1-5 which indicate promising oral availability. All the compounds except **5** are found to have drug-like molecular (DLM) properties and the probability to be lead candidates.

< Insert Tables 1 and 2 >

3.2. Absorption, Distribution, Metabolism and Excretion (ADME) properties

To be an efficient drug, the compound should have high biological activity in lower effective concentration with low toxicity and should be active until the desired action takes place. The drug discovery procedure takes the ADME properties of drug candidates into consideration for better pharmacokinetic profile. The pharmacokinetic properties can be calculated *in silico* using online databases like SwissADME (http://www.swissadme.ch/) [69] and pkCSM (http://biosig.unimelb.edu.au/pkcsm/) [70]. The ADME properties of indole chalcones are given in **Table 3**. Drug absorption was evaluated using solubility measurement and intestinal permeability. The aqueous solubility of the compounds is given as the logarithm of molar concentration and the solubility of designed compounds ranges from -2.90 to -6.045. The compounds are moderately water-soluble due to the presence of lipophilic functionalities aimed at improved cell permeability. As the absorption of an orally administrated drug occurs mostly through the small intestine, the percentage absorption of the compounds was evaluated. In general, Caco-2 permeability can predict the intake of oral drugs as Caco-2 from human colon carcinoma resemble intestinal epithelial cells. It is important to mention that the compound should have Papp > 8 $x10^{-6}$ cm/s for high permeability. Interestingly, all the compounds show high cell permeability remarkably higher than the standard Tb drugs such as INH and RIF. All the compounds except **16** show high intestinal absorption in the range of 90-95% which is twice that of RIF. The presence of hydrophilic hydroxy group and higher molecular weight of **16** renders the absorption of the drug by the intestine. INH shows 96% intestinal absorption which is slightly higher than all the indole chalcones. However, **15** showed intestinal absorption similar to INH at 95%.

The distribution profile of the drug was predicted using a volume of distribution (VDss), fraction unbound and blood-brain barrier permeability. Higher VDss indicates better distribution of the drug in the tissues than in plasma, and if Log VDss > 0.45 it shows the greater distribution in the tissues. All the compounds are moderately distributed in the tissues, they show better distribution than INH with compound **24** showing a higher range of 0.677. RIF is highly distributed in tissues with a value of 1.49 which is much higher than all the designed indole chalcones. Efficacy of drug calculated by fraction bound indicates that it is less bound to blood proteins and is free to diffuse. The blood-brain barrier (BBB) permeability was calculated by both SwissADME and pkSCM. The importance of BBB permeation is in affecting the central nervous system as in tuberculosis meningitis. Trifluoromethyl derivatives and nitro derivatives are unable to cross BBB similar to the standard drugs, INH and RIF. All the compounds interact with cytochromes either as substrates or as inhibitors while INH and RIF do not show any of these interactions. The total clearance of drugs (both hepatic and renal) was also studied and all the indole chalcones show a lower total clearance of -0.091 – 1.045 logml/min/kg. The compound **16** shows a total clearance of 0.688 logml/min/kg similar to INH and **17** is showing a total clearance of 1.045 logml/min/kg much higher than both INH and RIF. It can be concluded that all the compounds show good ADME properties in comparison with INH and RIF and can be considered as probable lead candidates.

<Insert Table 3>

3.3. Synthesis and characterization of indole chalcones

As the compounds are found to possess DLM properties and show good ADME properties, the designed indole chalcones are synthesized by aldol condensation as depicted in **Scheme 1**. Using the literature procedure [40, 71], indole-3-carboxaldehyde was reacted with

different substituted acetophenones to yield corresponding chalcones through Claisen–Schmidt condensation. The synthesized compounds were characterized by spectroscopic techniques like NMR, FT-IR and Mass spectrometry. The characteristic peak of C=C bond of chalcones appears as doublets, between 7-8 ppm in 1H NMR spectra, and at 125 ppm and 147 ppm in 13C NMR spectra. The NH protons of indole appear between 10-12 ppm in ^{1}H NMR spectra. The disappearance of methyl protons from acetophenone further confirms the formation of the expected product. In FT-IR spectra, the characteristic -NH stretching vibrations appeared around 3400 cm^{-1}, stretching vibrations of -C=C in conjugation with C=O appeared around 1600 cm^{-1} and carbonyl stretching vibrations appeared at 1700 cm^{-1}. The mass spectroscopy results show that the experimental molecular weight values are matching precisely with the theoretical molecular weight values.

< Insert Scheme 1>

3.4. Single crystal X-ray Diffraction analysis

The stereochemical arrangement of compounds can affect the drug-like properties and hence the exact configuration of compounds should be determined for the present indole chalcones as they can have either *Z* or *E* configuration. The single crystals of three compounds (**7, 11, 12**) crystallized in DMSO were selected as representative compounds. The solved single-crystal XRD patterns of the representative compounds are given in **Fig. 2**. The XRD data show that C=O and C=C group exist in *E* configuration and compounds are planar. The packing diagrams of **7, 11, 12** show the presence of intermolecular hydrogen bonding between different crystals of the same compound. The hydrogen bonding exists between N of -NH group of indoles of one crystal and O of -C=O of another crystal is at a distance of 1.977 Å, 2.021 Å, and 1.985 Å for **7, 11, 12**. respectively. The presence of hydrogen bonding stabilizes

the crystal structure in crystal packing and in the case of **7** and **12**, in a single unit-cell, the compounds are arranged in head to tail overlap with a length of 3.370 Å and 3.406 Å respectively. The compound **11** shows a displaced head to tail overlap in a unit cell and the crystal parameters of the three compounds are given in **Table 4.**

<Insert Fig. 2 and Table 4>

3.5. *In vitro antimycobacterial activity of indole chalcones*

After successful synthesis and characterization of indole chalcones, they were analyzed for *in vitro* antitubercular activity against $H_{37}Rv$ strain of *MTb*. Here, minimum inhibitory concentration (MIC) of indole-chalcones that yield 50% inhibition using LRP assay was considered to possess antitubercular activity. Rifampicin, the Group D Tb drug is considered the reference compound in the present investigation. The results of *in vitro* analysis are presented in **Table 2** along with the pharmacokinetic analysis data. The activity was afflicted by the presence of different substituents in conjugation with chalcones. The different heterocyclic substituents showed moderate to good activity with 65% to 85% inhibition having MIC values from 155 µM to 189 µM.

The substituted phenyl indole chalcone, **1** with fluorine substitution shows moderate activity with less than 55% inhibition at both 100 µg/ml and 50 µg/ml concentrations with MIC value of 188 µM. The possibility of fluorine being an active substituent was further explored by introducing trifluoromethyl groups in para and meta positions of phenyl ring (**2** and **3**). The trifluoromethyl groups were inactive with less than 30% inhibition of mycobacterium. Similarly, the introduction of chloro group (**4**) in para position of phenyl ring did not show much difference in activity with only 50% inhibition at 100 µg/ml and the inhibition further decreased with lowering of concentration. The attachment of Cl group at ortho-para positions

of phenyl moiety (as in **5**) showed an insignificant increase with more than 50% inhibition at both concentrations with MIC value of 164 µM. The activity of halo-substituents was further studied by introducing bromo substituent at the para position as in compound **6**. Surprisingly, the compound **6** showed 65% inhibition in 50 µg/ml concentration. The bromo group emerged as the most active group among the halo substituted compounds with MIC value of 155 µM. The inhibitory potential of halo substituted compounds are as follows: 4-Br>2,4 di-Cl> 4-F> 4-Cl> CF_3. The analysis shows that two compounds (**5** and **6**) hindered the growth of *Mycobacterium* at a concentration not more than 50 µg/ml. The introduction of the nitro group at the meta position (**7**) had no effect with compound showing merely 50% inhibition albeit at a higher concentration of 100 µg/ml. Furthermore, the bioisosteres of different substituents were considered for *in vitro* analysis The bioisostere of fluorine substituent, a hydroxy group (**8**) showed MIC value of 189 µM at 50 µg/ml with activity similar to the compound **1**. However, another bioisostere, amino group (**9**) shows no activity with less than 50% inhibition. The bioisostere of Cl, a methyl group (compound **10**) also showed similar activity with only 50% inhibition at 100 µg/ml concentration. Methoxy substitution as in **11** and **12** is also inactive against the bacterium. **Fig. 3a** shows the correlation between phenyl substituents and mycobacterial activity of indole chalcone derivatives. We observed that, based on resonance, the presence of electron-withdrawing groups in substituted phenyl ringsof indole chalcones augmented the antimycobacterial inhibition. Also, from the decreasing inhibitory potential of halo substituted compounds, it can be concluded that there has been an influence of the size of substituents on activity. All the halogens by means of inductive effect can attract the electrons from other atoms and the inductive effect will create a dipole moment within the compound. This can enhance the water solubility and enables the interaction of a drug with the biological target. The exception of hydroxyl group being active despite being an electron-donating group can be associated with its H-bond forming ability with the target. Here 7 compounds show promising inhibition at 100ug/ml with more than 50% inhibition of *Mycobacterium*, and 4

compounds show inhibition at even lower concentration of 50 µg/ml. Among phenyl substituted indole chalcones, compound **6** emerged as a promising candidate with MIC of 155 µM.

The library was further expanded by introducing heterocyclic scaffolds substituting phenyl ring. Different acetyl pyridines were introduced (**13, 14, 15**) which showed promising activity. Among these, the presence of 3-pyridine (**14**) showed higher activity with 70% inhibition at 100 µg/ml and all the pyridine derivatives showed MIC value of 201 µM. We noticed that the replacement of the pyridine ring with hydroxy phenyl piperazine (**16**) increased the activity at 100 µg/ml and displayed moderate inhibition of 65% at 50 µg/ml. The compound **16** displayed lower MIC value of 143 µM when compared to the pyridine substituents. This may be due to the presence of an additional -OH group capable of forming H-bonding. The introduction of 1-phenyl imidazole (**17**) in place of the 3-pyridine system did not affect the activity. Both **14** and **17** showed similar activity against $H_{37}Rv$ strain with MIC of **17** being slightly lower at 159 µM. In case of **17**, lowering the concentration from 100 µg/ml to 50 µg/ml had no perceivable effect in bacterial growth inhibition. The presence of furan (**18**) showed exceptionally high activity with more than 85% inhibition in both 100 µg/ml and 50 µg/ml concentrations. The most striking aspect of compound **18** is the negligible difference of 2% inhibition with change in concentration from 100 µg/ml to 50 µg/ml . A similar trend was observed for 2-thiophene moiety (20), with a slight difference of 5% in inhibition with change in concentration from higher to lower value. However, 3-thiophene (**21**) when compared to **20** showed lower inhibition of 60%. Both **20** and **21** showed lower MIC values of 197 µM compared to furan (**18**) counterpart. Surprisingly, one of the more prominent heterocyclic rings, 2-pyrrole (**19**) showed disappointing results with no inhibition even at higher concentration. Higher activity among N-containing rings is well connected to their increasing basicity. The basicity order and activity of N-rings are as follows: Piperazine>Imidazole>Pyridine>Pyrrole. Among the three pyridine derivatives, 3-pyridyl derivative (**14**) showed higher activity

followed by 4-pyridyl (**13**) and 2-pyridyl (**15**) derivatives. In 3-pyridyl derivative (**14**), C=O group in meta position acts as a deactivating substituent while in the case of 4-pyridyl and 2-pyridyl derivatives, C=O group in para and ortho positions respectively act as a slightly activating substituent. This can decrease the inductive effect of C=O group thereby decreasing the basicity of pyridine derivatives. Hence, the basicity order of pyridine derivatives follows the order: 3-pyridyl derivative (**14**) > 4-pyridyl (**13**) > 2-pyridyl (**15**) which is reflected in their activity. Aliphatic piperazine (**16**) is showing high basicity and hence shows 76% inhibition followed by aromatic counterparts. Pyrrole (**19**) being least basic shows no inhibition and similarly, furan (**18**) shows more activity than thiophene due to its higher basicity. As the ring size decreases, the activity is found to increase. The bioisosteres of pyridine (furan, thiophene and imidazole) showed higher activity and emerged as promising scaffolds in drug development. **Fig. 3b** shows the effect of heterocyclic substitution on the antimycobacterial activity of indole chalcones.

Moving onto fused heterocyclic systems, introduction of 1,3- benzodioxole (**22**) adjacent to chalcone moiety has shown promising inhibition with better MIC value of 171 µM. **22** shows good inhibition at 100 µg/ml and a moderate growth inhibition of 66% at 50 µg/ml . Napthyl group (**23**) however showed no inhibition. We have introduced two cyclic keto functionals adjacent to chalcones to study their influence in activity. Aliphatic cyclopentanone group (**24**) showed relatively higher result with more than 85% inhibition with MIC value of 236 µM. The replacement of cyclopentanone with larger cyclohexanone moiety (**25**), however, reduced the inhibition to 53% with MIC of 221 µM. The effect of fused heterocyclic and aliphatic systems on the anti-mycobacterial activity is shown in **Fig. 3c**. Heterocyclic compounds showed Log P values in the range of 2.49 - 3.68. The relatively low Log P values indicate the higher lipophilicity of compounds and hence easier cell permeability. The effect of Log P values on the MIC of *MTb* is given in **Fig. 4.**

<Insert Fig. 3 and Fig. 4 >

The structure activity relationship is explained in terms of bioisosteres which are used in drug design for improving pharmacological activity, improved target selectivity and reducing the side effects. The different bioisosteres employed in the current study are described in **Table 5** with corresponding Log P and MIC values. The substituted phenyl indole chalcone, **1** with fluorine substitution shows moderate activity with MIC value of 188 µM and Log P value of 3.65. When fluorine is replaced by its bioisosteres, hydroxy (**8**) and amino (**9**) groups, there is a decrease in Log P values with decreasing inhibition of bacterial growth. A similar trend is followed when chloro (**4**) and bromo (**6**) substitutions are replaced with hydroxy group. In both cases, electron withdrawing groups in para position of phenyl ring emerged as more potent for inhibiting the bacterial growth. Electron donating group in para position instead of electron withdrawing group shows diminishing inhibition as seen by replacing chlorine with its bioisostere methyl (**10**). The presence of dichloro substitution as in compound **5** is more efficient than p-chloro substitution despite the violation of Lipinski rule regarding Log P. The trifluoromethyl group, the bioisostere of halogens was inactive with less than 30% inhibition compared to **1, 4, 6**. The bromo group (**6**) emerged as the most active group among the halo substituted compounds and their bioisosteres with MIC value of 155 µM which can be attributed to electron withdrawing efficiency and larger size of bromo substitution. Different acetyl pyridines (**13, 14, 15**) showed promising activity with 3-pyridine (**14**) showing higher activity with 70% inhibition at 100 µg/ml and all the pyridine derivatives showed MIC value of 201 µM. The pyridine ring was replaced with their bioisosteres furan and thiophene to check their inhibitory potential. The presence of furan (**18**) showed exceptionally high activity with >85% inhibition at both concentrations with a difference of 2% in inhibition from change in concentration from 100 µg/ml to 50 µg/ml. 2-thiophene moiety (**20**) showed similar trend but with slight difference of 5% in inhibition rate with change in concentration. However, 3-

thiophene (**21**) showed lower inhibition than all other bioisosteres of pyridine except for 2-pyridine derivative (**15**). Furan (**18**) shows more activity due to its higher basicity and as the ring size decreases, the activity is found to increase.

< Insert Table 5 >

From the above discussions, it can be summarized that the heterocyclic compounds showed higher activity in LRP assay and turned out to be promising scaffolds for further modifications. The activity was associated with the size and basicity of the heterocyclic rings. Five membered rings show better activity than six-membered rings owing to their small size and hence better cell permeability. Among all the compounds, **18, 24** and **20** emerged as most active compounds with higher inhibition of mycobacterium and MIC values ranging from 170 µM to 210 µM. These compounds exhibit higher inhibition at 50 µg/ml which is similar to clinically used PZA showing anti-Tb activity of 50 µg/ml at pH 5.5 and 400 ug/ml at pH 5.95 [72]. The studies reveal that indole-chalcone compounds are promising starting points for drug candidates and must be further explored for their potential .

3.6. Docking studies

The successful synthesis and antitubercular properties of some of the indole chalcones prompted us to explore the binding of the compounds to plausible molecular targets. The aforementioned studies helped to identify active lead compounds, **18**, **20**, **24.** Molecular docking studies were performed to recognize the potential target for inhibiting *MTb*. In order to pin down the mode of binding as well as binding affinities, a suitable protein target should first be selected. Several well-known anti-tubercular drug-receptors were selected for blind docking and are listed as follows: mycolic acid transporters (PDB: **6AJH**) [73], DNA gyrase (PDB:

3IFZ) [74], GyrB ATPase (PDB: **4B6C**) [75], long-chain enoyl-acyl carrier protein reductase (PDB: **1ZID**) [76], oxidoreductase DprE1 (PDB: **4FDO**) [77], cytochrome P450 (PDB: **1N40**) [78], β-ketoacyl synthase KasA (PBD: **2WGD**) [79].

The *in silico* results which best fit the in-vitro observations (KasA protein, PDB: **2WGD**) were analyzed post-docking to identify interacting amino acid groups and were compared with previously studied mechanisms. KasA protein (PDB ID: **2WGD**) inhibition is long known to suppress the *MTb* disease [80]. KasA protein is essential to the cell wall synthesis of *MTb* and inhibition of this protein by a molecule could be an indicator of its nature as an anti-Tb agent. The *in silico* results of the compounds against KasA protein are given in **Table 6**. Compound **20** displayed a binding affinity of -6.5 kcal mol^{-1} and it shows interactions with GLU-40 (electrostatic interactions of N on GLY with indole rings of **20**), SER-41 (H-bonding of NH of **20** to C=O of SER), GLU-224 (H-bonding of GLU OH with C=O of **20**) and LEU-371 (hydrophobic interactions with thiophene present in **20**). Compound **24** has a binding strength of -6.9 kcal mol^{-1} and it shows interactions with GLU-40 (electrostatic interaction of indole ring with N of GLU), LEU-371 and ARG-225 (both show hydrophobic interactions with cyclopentanone). Similarly, compound **18** shows binding affinity of -7.9 kcal mol^{-1} and interacts with THR-313 (H-bonding of C=O of **18** and OH on THR), HIS-311 (electrostatic and hydrophobic interaction between furan of **18** and imidazole of HIS). VAL-278, ALA-215, ALA-279, PRO-280 and ILE-317 also showed hydrophobic interactions with indole moiety present in **18**. Post analysis it was noted that compounds **20** and **24** interacted with two of the same amino acids namely GLU-40 and LEU-371. What was most interesting was that **18** showed high binding affinity to KasA protein as well as its binding mode was similar to known FAS-II inhibitors such as INH and Thiolactomycin [80]. The compound **18** displayed the highest inhibition of *MTb* among the synthesized compounds and the specific interactions of **18** with KasA protein are shown in **Fig. 5**. The interactions of **18** with HIS-311 (a member of the

catalytic triad), VAL-278, ALA-279 and PRO-280 and its proximity to PHE-404 which is a gatekeeper to the acyl channel present in KasA protein are the likely the causes for its efficacy in *MTb* inhibition. Due to this, compound **18** may prove to be a useful candidate against INH resistant *MTb* strains and could prove to be a valuable starting point for new anti-tubercular drugs.

<Insert Table 6 and Fig. 5>

3.7. Plausible mechanism of action

The metal chelation is important in Tb infection as *MTb* needs iron to grow inside the host organism. The bacteria take iron from the host and hence, withholding the supply of iron can, in turn, reduce the multiplication of bacteria. Iron chelators can reduce bacterial growth either by withholding iron or by forming free radicals which may be toxic to bacteria [81, 82]. The iron chelator should be permeable to the cell membrane and hence, the presence of lipophilic functional groups is important. In chalcone, the carbonyl oxygen and other heteroatoms can act as electron donors to form complexes with metal atoms. The properties of chalcones such as smaller size, higher charge density, higher stability and presence of electron-donating heteroatoms in the ring allow for the chelation of metals. This can have a considerable role in the improved activity of chalcones. The importance of metal chelation can be explained by overtone concept of cell permeability and Tweedy's theory of chelation. As stated by overtone theory, cellular membranes are made up of lipids and allow the entry of lipophilic molecules only. Chalcones can chelate metal ions reducing the polarity of metal ions by the overlap of ligand orbital and metal orbital. The π-electrons are delocalised on chelating ring augmenting the complex to enter into the cell membranes. This can block the binding sites for metal which is important for the bacterium itself [83], hence increasing antimycobacterial

properties of the metal chalcone complexes. The presence of heterocycles in conjugation with the carbonyl oxygen further strengthens the possibility of metal chelation by donating the lone pair of electrons. The possible binding modes of chalcones with metal [84] are shown in **Fig. 6**.

<Insert Fig. 6>

3.8. Evaluation of cytotoxicity

Compounds (*E*)-1-(furan-3-yl)-3-(1*H*-indol-3-yl)prop-2-en-1-one (**18),** (*E*)-3-(1*H*-indol-3-yl)-1-(thiophen-2-yl)prop-2-en-1-one **(20)** and (*E*)-2-((1*H*-indol-2-yl)methylene)cyclopentan-1-one (**24)** were tested for cytotoxicity in human megakaryocyte cell line (Mo7e) and Murine pro B cell line (BA/F3). Compounds which inhibit more than 50% cell growth were considered to be cytotoxic to cells. We observed that more than 80% cell viability in a human megakaryocyte cell line, Mo7e when treated with compounds **18**, **20** and **24**. Similarly, in murine Pro B cell line BA/F3, cell viability of more than 60% was observed when treated with compounds **18, 20** and **24**. Overall the results suggest that the compounds **18, 20** and **24** are not cytotoxic to human megakaryocytes and murine B cells. Percentage cell viability of Mo7e and BA/F3 cells against test compounds **18, 20** and **24** is given in **Fig. 7**.

<Insert Fig. 7>

4. Conclusion

A library of indole chalcone derivatives was synthesized and its potency against $H_{37}Rv$ strain of *M.Tb* is studied. Among these, 3 compounds , (*E*)-1-(furan-3-yl)-3-(1*H*-indol-3-

yl)prop-2-en-1-one (**18), (***E*)-3-(1*H*-indol-3-yl)-1-(thiophen-2-yl)prop-2-en-1-one **(20)** and (*E*)-2-((1*H*-indol-2-yl)methylene)cyclopentan-1-one (**24)** were found to be potential drug candidates against tuberculosis with MIC of 210, 197, 236 µM respectively. The activity is linked to the size of the heterocyclic ring and their ability to chelate metal atoms vital to mycobacterium. The docking studies run to comprehend the binding manner of indole chalcones indicate that compound **18** showed binding modes similar to FAS-II inhibitors like INH or Thiolactomycin against KasA protein. Cytotoxicity assay results suggest that the compounds **18, 20** and **24** are noncytotoxic to human megakaryocytes and murine B cells. Compound **20** is showing high potential against *MTb* with lower cytotoxicity. Overall, the studies reveal that the compounds show potential as an important drug backbone against Tb. The structural modifications for enhancement in anti-mycobacterial activity is worth exploring and is under progress in our laboratory.

Acknowledgement

Deepthi Ramesh thanks DST for DST-INSPIRE fellowship (JRF). Authors thank University Grants Commission (UGC), New Delhi for their financial support under Special Assistance Program, stage DSA-I to Department of Chemistry, Pondicherry University (No. F.540/6/DSA-1/2016/(SAP-1) dated 31-10-2018). Authors thank S. Anbarasu, Sathyabama University, Chennai, India for mycobacterial studies, Central Instrumentation Facility (CIF), Pondicherry University for spectral analysis. The authors also thank Binoy Saha, Arjith Saha, Department of Chemistry, Pondicherry University for XRD characterization, and Ramkishore Matsa, Department of Chemistry, Pondicherry University for his timely help.

Figures and Scheme legends

Fig. 1. (a) Indole drugs in a clinical trial for MDR-Tb (b) Biologically active indole-chalcones in literature**.**

Fig. 2. Single-crystal XRD data. The ORTEP diagrams (a, d, g), Packing diagrams (b, e, h) and Hydrogen bond interaction diagrams (c, f, i) of compounds **7, 11, 12.**

Fig. 3. Correlation diagram of percentage inhibition with differently substituted indole chalcones.

Fig. 4. Effect of Log P values of indole chalcones against the MIC values.

Fig. 5. Post docking analysis (a) KasA protein interaction with **18** (b) Ligand receptor interactions of KasA and **18** (c) 2-D interaction diagram of **18** with KasA.

Fig. 6. (a) and (b) show two different binding modes of chalcones with metal, (c) shows a binding mode of chalcone with heterocyclic groups and (d) shows the presence of back bonding in heterocyclic chalcones causing chelation increasing lipophilicity and activity.

Fig. 7. Percentage cell viability of Mo7e and BA/F3 cells against test compounds **18**, **20** and **24**. (a) Mo7e cells and (b) BA/F3 cells were stimulated with indicated concentrations of

compounds **18**, **20** and **24** for 24 h. Cytotoxicity of cells was studied using WST-1 assay. Data are represented as mean ± s.e.m. P value is calculated using student t-test. *P < 0.05.

Scheme 1: Synthesis of indole chalcone derivatives.

Table 1: Library of Indole chalcone derivatives

Category I: Substituted phenyl indole chalcone derivatives (1-12)

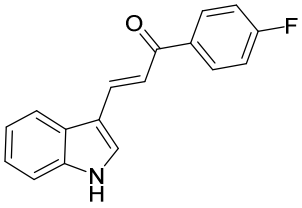

1

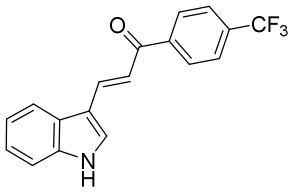

2

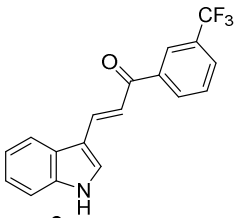

3

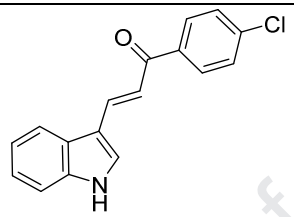

4

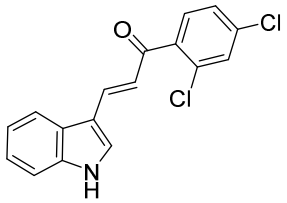

5

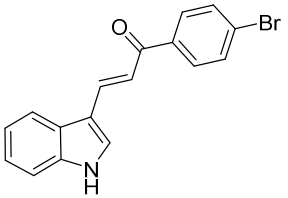

6

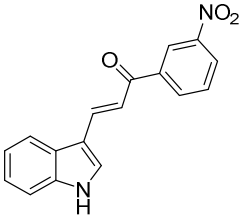

7

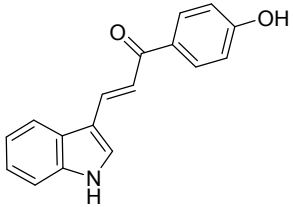

8

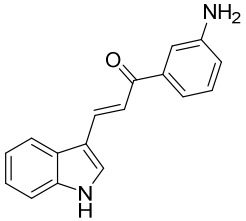

9

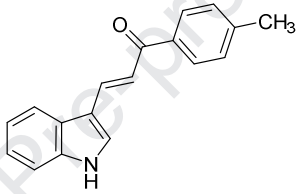

10

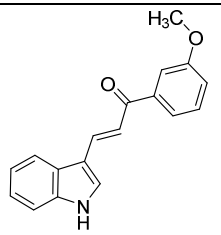

11

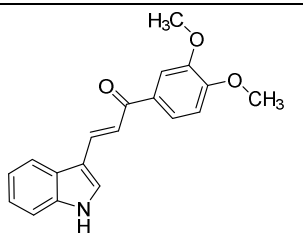

12

Category II: Six-membered heterocyclic indole chalcones (13-16)

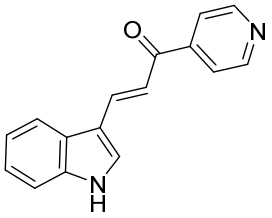

13

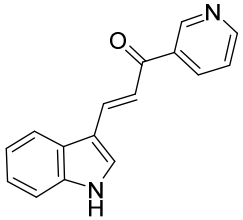

14

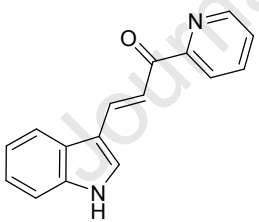

15

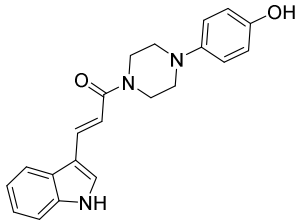

16

Category III: Five-membered heterocyclic indole chalcones (17-21)

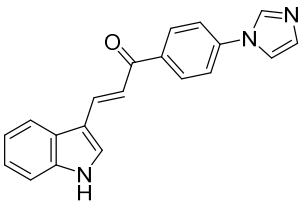

17

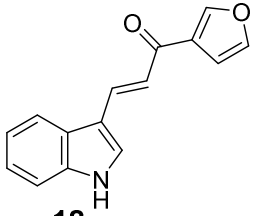

18

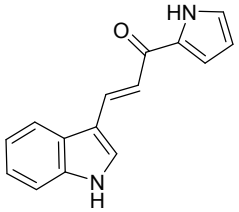

19

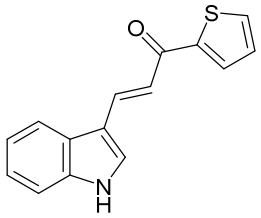

20

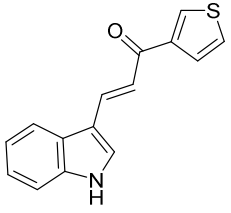

21

Category IV: Fused indole chalcones (22-23)

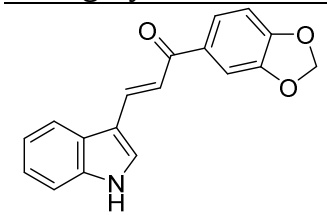

22

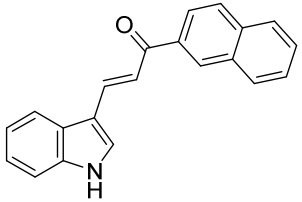

23

Category V: Aliphatic indole chalcones (24,25)

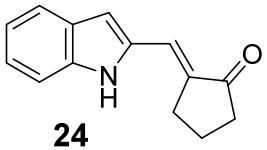

24

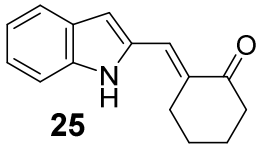

25

590 **Table 2: Pharmacokinetic analysis and *in vitro* mycobacterial analysis result of indole**

591 **chalcones**

	Lipinski's Rule of 5					Veber Rule		% Inhibition		MIC against *MTb* (µM)
Code.	**Log P**	**Mol. Wt**	**H donor**	**H acceptor**	**No of violations**	**TPSA (Å^2)**	**No. of rotatable bonds**	**100 µg/ml**	**50 µg/ml**	
1.	3.65	265.29	1	2	0	32.86	3	54.25	50.26	188
2.	4.68	315.29	1	2	0	32.86	4	31.17	29.68	> 317
3.	4.68	315.29	1	2	0	32.86	4	26.31	24.52	> 317
4.	4.46	281.74	1	2	0	32.86	3	50.65	48.65	>355
5.	5.07	316.19	1	2	1	32.86	3	55.16	52.26	164
6.	4.59	326.19	1	2	0	32.86	3	65.86	64.86	155
7.	3.72	292.29	1	5	0	78.69	4	51.73	48.70	> 342
8.	3.30	263.30	2	3	0	53.09	3	55.12	54.9	189
9.	2.83	262.31	3	3	0	58.88	3	48.7	37.24	> 381
10.	4.23	261.32	1	2	0	32.86	3	50.85	41.68	> 382
11.	3.81	277.32	1	3	0	42.10	4	36.68	27.12	> 360
12.	3.43	307.35	1	4	0	51.33	5	31.69	27.05	> 325
13.	2.49	248.28	1	3	0	45.75	3	64.2	58.35	201
14.	2.49	248.28	1	3	0	45.75	3	70.72	63.09	201
15.	2.61	248.28	1	3	0	45.75	3	62.05	53.10	201
16.	3.10	347.42	2	5	0	59.57	3	76.44	63.83	143
17.	3.11	313.36	1	4	0	50.69	4	70.73	63.57	159
18.	2.73	237.26	1.	3	0	46.00	3	87.67	85.34	210
19.	2.94	236.27	2	3	0	48.65	3	49.37	26.38	> 423

20.	3.68	253.33	1	2	0	32.86	3	87.18	81.97	197
21.	3.37	253.33	1	2	0	32.86	3	63.38	62.05	197
22.	3.98	291.31	1	4	0	51.33	3	75.72	66.76	171
23.	4.94	297.36	1	2	0	32.86	3	41.83	30.8	> 336
24.	2.96	211.26	1	2	0	32.86	1	86.34	84.29	236
25.	3.47	225.29	1	2	0	32.86	1	61.97	53.07	221
INH	-0.96	137.14	3	4	0	68.01	1	> 99%		1.4 (2 µg/ml)
RIF	2.62	822.95	6	16	3	220.16	5	> 99%		2.4 (2 µg/ml)

592

593 Note: Pharmacokinetic analysis are obtained from the Molinspiration server

594 (http://www.molinspiration.com)

595

596 **Table 3: ADME properties of indole chalcones**

Code	Absorption			Distribution				Metabolism	Excretion
	Log S (log mol/L)	Caco-2 perm. (log Papp in 10^{-6} cm/s)	Int. abs. (% Absorbed)	VDss (log L/kg)	Fract. Unb (Fu)	BBB perm (log BB)	BBB pred		Total clearance (logml/min/kg)
1.	-4.71	1.802	92.088	0.241	0.038	0.29	Yes	CYP2D6, CYP3A4 substrate. CYP1A2, CYP2C19, CYP2C9, CYP2D6 inhibitor	0.249
2.	-5.098	1.592	91.295	0.356	0.017	0.251	No	CYP3A4 substrate. CYP1A2, CYP2C19, CYP2C9, CYP3A4 inhibitor	0.171
3.	-5.11	1.59	92.161	0.383	0.019	0.23	No	CYP3A4 substrate. CYP1A2, CYP2C19, CYP2C9, CYP3A4 inhibitor	0.182
4.	-4.711	1.615	92.498	0.347	0.031	0.268	Yes	CYP3A4 substrate. CYP1A2, CYP2C19, CYP2C9, CYP3A4 inhibitor	-0.091
5.	-5.217	1.627	91.274	0.416	0.002	0.255	Yes	CYP2D6, CYP3A4 substrate. CYP1A2, CYP2C19, CYP2C9, CYP3A4 inhibitor	0.024
6.	-5.093	1.685	91.166	0.395	0.015	0.276	Yes	CYP2D6, CYP3A4 substrate. CYP1A2,	-0.112

								CYP2C19, CYP2C9, CYP3A4 inhibitor	
7.	-4.647	0.804	92.966	0.272	0.017	-0.14	No	CYP3A4 substrate. CYP1A2, CYP2C19, CYP2C9, CYP3A4 inhibitor	0.411
8.	-3.873	1.33	91.274	0.151	0.072	0.037	Yes	CYP3A4 substrate. CYP1A2, CYP2C19, CYP2C9, CYP2D6 inhibitor	0.345
9.	-4.017	1.308	92.61	0.418	0.078	-0.087	Yes	CYP3A4 substrate. CYP1A2, CYP2C19, CYP2C9, CYP3A4 inhibitor	0.409
10.	-4.7	1.518	93.13	0.275	0.039	0.319	Yes	CYP2D6, CYP3A4 substrate. CYP1A2, CYP2C19, CYP2C9, CYP2D6, CYP3A4 inhibitor	0.384
11.	-4.545	1.714	93.963	0.148	0.044	0.157	Yes	CYP3A4 substrate. CYP1A2, CYP2C19, CYP2C9, CYP3A4 inhibitor	
12.	-4.812	1.376	95.374	0.355	0.046	0.105	Yes	CYP3A4 substrate. CYP1A2, CYP2C19, CYP2C9, CYP3A4 inhibitor	0.408
13.	-3.649	1.372	94.71	0.015	0.142	0.278	Yes	CYP3A4 substrate.	0.451

								CYP1A2, CYP2C19, inhibitor	
14.	-3.661	1.362	94.71	-0.038	0.149	0.273	Yes	CYP3A4 substrate. CYP1A2, CYP2C19, inhibitor	0.443
15.	-3.555	1.349	95.081	-0.137	0.191	0.337	Yes	CYP3A4 substrate. CYP1A2, CYP2C19, inhibitor	0.307
16.	-4.186	1.023	89.456	0.208	0.052	0.097	Yes	CYP2D6, CYP3A4 substrate. CYP1A2, CYP2C19, CYP2C9, CYP3A4 inhibitor	0.688
17.	-2.923	1.396	90.611	0.287	0.022	0.261	Yes	CYP3A4 substrate. CYP1A2, CYP2C19, CYP2C9, CYP2D6, CYP3A4 inhibitor	1.045
18.	-3.771	1.353	93.39	0.061	0.148	0.248	Yes	CYP2D6, CYP3A4 substrate. CYP1A2, CYP2C19 inhibitor	0.405
19.	-3.66	1.291	91.393	0.057	0.23	0.30	Yes	CYP2D6 substrate. CYP1A2, CYP2C19, CYP2D6 inhibitor	0.455
20.	-4.434	1.679	90.897	0.19	0.045	0.314	Yes	CYP2D6, CYP3A4 substrate. CYP1A2, CYP2C19, CYP2C9 inhibitor	0.114
21.	-4.434	1.679	90.897	0.19	0.045	0.314	Yes	CYP2D6, CYP3A4 substrate. CYP1A2,	0.028

								CYP2C19, CYP2C9 inhibitor	
22.	-4.482	1.323	93.861	0.085	0.042	0.237	Yes	CYP3A4 substrate. CYP1A2, CYP2C19, CYP2C9, CYP3A4 inhibitor	0.257
23.	-6.045	1.695	92.541	0.02	0.08	0.318	Yes	CYP2D6, CYP3A4 substrate. CYP1A2, CYP2C19, CYP2C9, CYP2D6, CYP3A4 inhibitor	0.343
24.	-3.099	1.63	93.421	0.677	0.256	0.416	Yes	CYP3A4 substrate. CYP1A2, CYP2C19, inhibitor	0.285
25	-3.591	1.654	92.479	0.404	0.2	0.4	Yes	CYP3A4 substrate. CYP1A2, CYP2C19, inhibitor	0.297
INH	-2.024	0.695	96.452	0.053	0.776	-0.002	No	-	0.703
RIF	-2.914	-0.219	41.095	1.49	0.209	-2.577	No	-	-0.624

NOTE: The pharmacokinetic properties are calculated *in silico* using online databases like SwissADME (http://www.swissadme.ch/) and pkCSM (http://biosig.unimelb.edu.au/pkcsm/).

600 **Table 4: Single-crystal XRD data**

601

	Compound **7**	Compound **11**	Compound **12**
CCDC Number	1988479	1988481	1988480
Empirical formula	$C_{17}H_{12}N_2O_3$	$C_{18}H_{15}NO_2$	$C_{19}H_{17}NO_3$
Formula weight	292.29	277.33	307.34
Temperature/K	298	298	298
Crystal system	monoclinic	monoclinic	triclinic
Space group	$P2_1/n$	$P2_1/c$	P-1
a/Å	7.4684(8)	7.2538(9)	7.4097(13)
b/Å	24.813(2)	22.917(2)	8.3495(19)
c/Å	8.1427(8)	9.1443(11)	13.317(3)
α/°	90.00	90	89.266(17)
β/°	110.558(13)	111.331(14)	85.961(15)
γ/°	90.00	90	67.969(19)
Volume/Å^3	1412.8(2)	1416.0(3)	761.7(3)
Z	4	4	2
ρ_{calc}g/cm^3	1.374	1.3008	1.340
μ/mm^{-1}	0.096	0.085	0.091
F(000)	608.0	584.3	324.0
Crystal size/mm^3	0.46 × 0.38 × 0.14	0.48 × 0.42 × 0.36	0.54 × 0.38 × 0.22
Radiation	MoKα (λ = 0.71073)	Mo Kα (λ = 0.71073)	MoKα (λ = 0.71073)
2Θ range for data collection/°	6.28 to 58.66	6.28 to 58.72	5.94 to 58.68

Index ranges	$-6 \leq h \leq 10, -33 \leq k \leq 31, -11 \leq l \leq 10$	$-9 \leq h \leq 9, -30 \leq k \leq 20, -12 \leq l \leq 11$	$-9 \leq h \leq 9, -11 \leq k \leq 10, -17 \leq l \leq 17$
Reflections collected	7950	7854	4737
Independent reflections	3289 [R_{int} = 0.0251, R_{sigma} = 0.0335]	3338 [R_{int} = 0.0313, R_{sigma} = 0.0503]	3076 [R_{int} = 0.0176, R_{sigma} = 0.0320]
Goodness-of-fit on F^2	1.021	1.030	1.036

602 **Table 5: Structure activity relationships of indole chalcones**

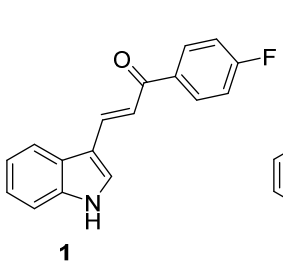 **1**	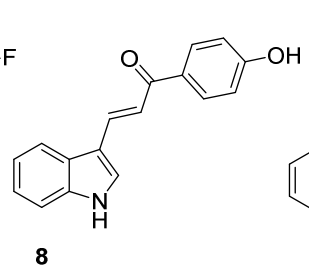 **8**	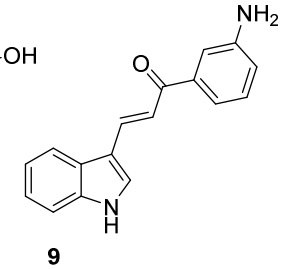 **9**	
Log P =3.65	Log P =3.30	Log P =2.83	
MIC = 189 µM	MIC = 188 µM	MIC = > 381 µM	
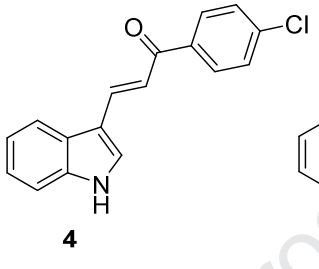 **4**	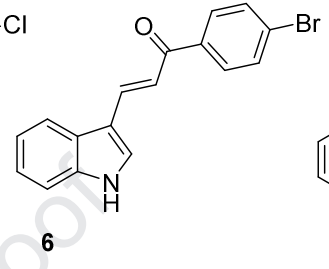 **6**	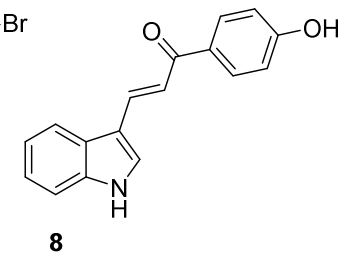 **8**	
Log P =4.46	Log P= 4.59	Log P= 3.30	
MIC = > 355 µM	MIC= 155 µM	MIC= 188 µM	
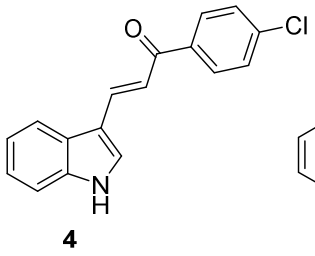 **4**	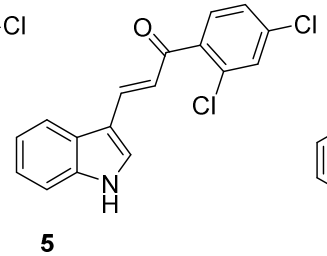 **5**	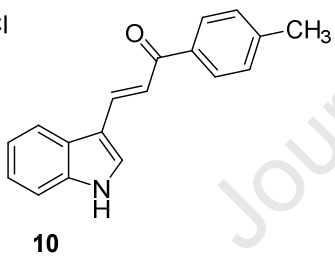 **10**	
Log P =4.46	Log P =5.07	Log P =4.23	
MIC = > 355 µM	MIC = 164 µM	MIC = > 382 µM	
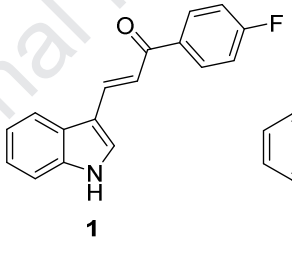 **1**	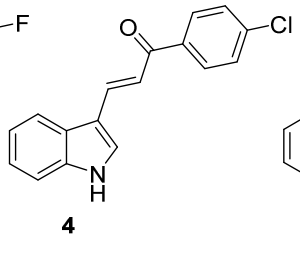 **4**	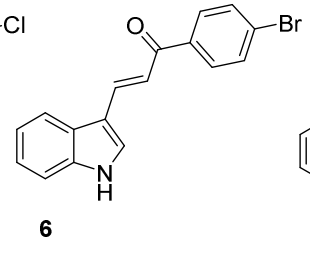 **6**	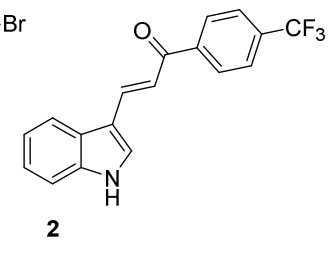 **2**
Log P =3.65	Log P =4.46	Log P =4.59	Log P =4.68
MIC = 188 µM	MIC = > 355 µM	MIC = 155 µM	MIC = > 317 µM

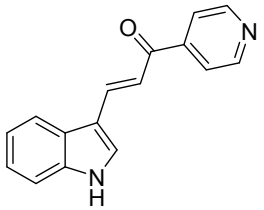 **13**	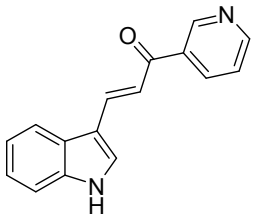 **14**	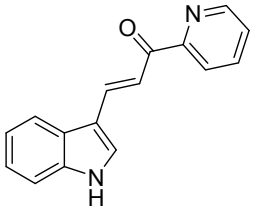 **15**	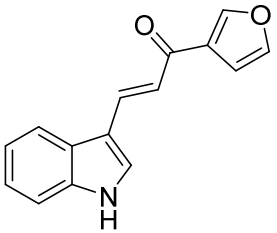 **18**	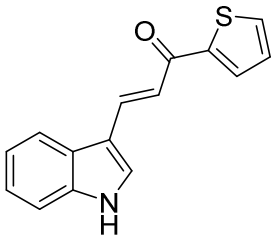 **20**	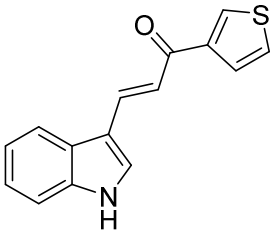 **21**
Log P =2.49	Log P =2.49	Log P =2.61	Log P =2.73	Log P =3.68	Log P =3.37
MIC = 201 µM	MIC = 201 µM	MIC = 201 µM	MIC = 210 µM	MIC = 197 µM	MIC = 197 µM

603

604

605

606

607

608

609

610

611 **Table 6: *In silico* studies with KasA protein**

***In silico* studies with KasA protein**			
Code	**Binding Affinity (kcal/mol)**	**Binding constant (Ki) (µM)**	**Interacting amino acids**
1	-7.3	4.39666	GLU224, GLU40, LEU371, SER41
2	-7.9	1.59526	GLU224, GLY387, GLU40, LEU371, SER41
3	-7.8	1.88892	GLU40, GLU224, ASN372, GLU40, GLU40, LEU371
4	-7.5	3.13588	GLU40, LEU371, GLU224, ASN372
5	-7.4	3.71314	LEU371, LEU371, HIS44, GLU224, ASN372
6	-7.5	3.13588	GLU224, GLU40, LEU371, SER41
7	-7.9	1.59526	HIS311, ILE317, GLY318, ASP319, MET213, ALA215, ALA279, PRO280
8	-7.1	6.16434	GLU40, SER41, LEU371
9	-7.3	4.39666	LEU371, SER41, GLU224, ASN372, GLU224
10	-7.5	3.13588	GLU40, LEU371, GLU224, ASN372
11	-7.3	4.39666	GLU224, GLU40, LEU371, SER41
12	-7.4	3.71314	GLU224, GLU40, LEU371, SER41, GLY39

13	-8.5	5.78816	THR313, HIS311, ILE317, ALA279, PRO280, ALA215
14	-7.1	6.16434	LEU371, ASN372, SER41, GLU224
15	-6.8	10.2337	LEU371, GLU224, ASN372, GLU224, SER41
16	-8.5	0.578816	GLY387, GLU40, ASN372, LEU371, THR370, TYR373, GLY39
17	-7.9	1.59526	GLU40, LEU371, THR370
18	-7.9	1.59526	THR313, HIS311, ILE317, ALA215, VAL278, ALA279, PRO280
19	-6.8	1.02337	GLU224, GLU40, LEU371, SER41, GLY39
20	-6.5	16.9894	GLU224, GLU40, LEU371, SER41
21	-6.6	14.3482	LEU371, GLU224, ASN372
22	-7.9	1.59526	GLU224, ASN372, GLU40, LEU371, SER41
23	-8.1	1.13781	GLU40, LEU371, PRO369, GLU224
24	-6.9	8.64272	GLU40, ARG225, LEU371
25	-6.9	8.64272	GLU40, ARG225, LEU371
INH	-6.1	33.3969	VAL 278, GLY 403, HIS 311, PRO 280
RIF	-7.8	1.88892	GLU 224, LEU 371

612

Appendix A. Supplementary data

The Supplementary data of this article is available online, at .

These data include the spectroscopic data of all the indole chalcones and *in silico* studies of indole chalcones against different Tb proteins described in the paper.

References

[1] Global tuberculosis report, in, World Health Organisation, 2019 Geneva.

[2] A. Campaniço, R. Moreira, F. Lopes, Drug discovery in tuberculosis. New drug targets and antimycobacterial agents, Eur. J. Med. Chem., 150 (2018) 525-545.

[3] S. Tiberi, A. Scardigli, R. Centis, L. D'Ambrosio, M. Muñoz-Torrico, M.Á. Salazar-Lezama, A. Spanevello, D. Visca, A. Zumla, G.B. Migliori, J.A. Caminero Luna, Classifying new anti-tuberculosis drugs: rationale and future perspectives, Int. J. Infect. Dis., 56 (2017) 181-184.

[4] D. Sharma, Y.K. Dhuriya, N. Deo, D. Bisht, Repurposing and revival of the drugs: A new approach to combat the drug resistant tuberculosis, Front. Microbiol., 8 (2017) 2452-2452.

[5] D.J.C. Knowles, New strategies for antibacterial drug design, Trends Microbiol., 5 (1997) 379-383.

[6] M.W. Majewski, R. Tiwari, P.A. Miller, S. Cho, S.G. Franzblau, M.J. Miller, Design, synthesis, and anti-tuberculosis activities of conjugates of piperazino-1,3-benzothiazin-4-ones (pBTZs) with 2,7-dimethylimidazo [1,2-a]pyridine-3-carboxylic acids and 7-phenylacetyl cephalosporins, Bioorg. Med. Chem. Lett., 26 (2016) 2068-2071.

[7] T. Yuan, N.S. Sampson, Correction to hit generation in Tb drug discovery: From genome to granuloma, Chem. Rev., 119 (2019) 7718-7718.

[8] S. Wellington, D.T. Hung, The expanding diversity of Mycobacterium tuberculosis drug targets, ACS Infect. Dis., 4 (2018) 696-714.

[9] S. Pajk, M. Živec, R. Šink, I. Sosič, M. Neu, C.-w. Chung, M. Martínez-Hoyos, E. Pérez-Herrán, D. Álvarez-Gómez, E. Álvarez-Ruíz, A. Mendoza-Losana, J. Castro-Pichel, D. Barros, L. Ballell-Pages, R.J. Young, M.A. Convery, L. Encinas, S. Gobec, New direct inhibitors of InhA with antimycobacterial activity based on a tetrahydropyran scaffold, Eur. J. Med. Chem., 112 (2016) 252-257.

[10] P. Pan, S.E. Knudson, G.R. Bommineni, H.-J. Li, C.-T. Lai, N. Liu, M. Garcia-Diaz, C. Simmerling, S.S. Patil, R.A. Slayden, P.J. Tonge, Time-dependent diaryl ether inhibitors of InhA: Structure–activity relationship studies of enzyme inhibition, antibacterial activity, and in vivo efficacy, ChemMedChem, 9 (2014) 776-791.

[11] L. Encinas, H. O'Keefe, M. Neu, M.J. Remuiñán, A.M. Patel, A. Guardia, C.P. Davie, N. Pérez-Macías, H. Yang, M.A. Convery, J.A. Messer, E. Pérez-Herrán, P.A. Centrella, D. Álvarez-Gómez, M.A. Clark, S. Huss, G.K. O'Donovan, F. Ortega-Muro, W. McDowell, P. Castañeda, C.C. Arico-Muendel, S. Pajk, J. Rullás, I. Angulo-Barturen, E. Álvarez-Ruíz, A. Mendoza-Losana, L. Ballell Pages, J. Castro-Pichel, G. Evindar, Encoded library technology as a source of hits for the discovery and lead optimization of a potent and selective class of bactericidal direct inhibitors of Mycobacterium tuberculosis InhA, J. Med. Chem., 57 (2014) 1276-1288.

[12] X. He, A. Alian, P.R. Ortiz de Montellano, Inhibition of the Mycobacterium tuberculosis enoyl acyl carrier protein reductase InhA by arylamides, Bioorg. Med. Chem., 15 (2007) 6649-6658.

[13] M.R. Kuo, H.R. Morbidoni, D. Alland, S.F. Sneddon, B.B. Gourlie, M.M. Staveski, M. Leonard, J.S. Gregory, A.D. Janjigian, C. Yee, J.M. Musser, B. Kreiswirth, H. Iwamoto, R. Perozzo, W.R. Jacobs Jr, J.C. Sacchettini, D.A. Fidock, Targeting tuberculosis and malaria

through inhibition of enoyl reductase. Compound activity and structural data, J. Biol. Chem., 278 (2003) 20851-20859.

[14] M.D. Wall, M. Oshin, G.A.C. Chung, T. Parkhouse, A. Gore, E. Herreros, B. Cox, K. Duncan, B. Evans, M. Everett, A. Mendoza, Evaluation of N-(phenylmethyl)-4-[5-(phenylmethyl)-4,5,6,7-tetrahydro-1H-imidazo[4,5-c]pyridin-4-yl]benzamide inhibitors of Mycobacterium tuberculosis growth, Bioorg. Med. Chem. Lett., 17 (2007) 2740-2744.

[15] J.R. Brown, E.J. North, J.G. Hurdle, C. Morisseau, J.S. Scarborough, D. Sun, J. Korduláková, M.S. Scherman, V. Jones, A. Grzegorzewicz, R.M. Crew, M. Jackson, M.R. McNeil, R.E. Lee, The structure–activity relationship of urea derivatives as anti-tuberculosis agents, Bioorg. Med. Chem., 19 (2011) 5585-5595.

[16] V. La Rosa, G. Poce, J.O. Canseco, S. Buroni, M.R. Pasca, M. Biava, R.M. Raju, G.C. Porretta, S. Alfonso, C. Battilocchio, B. Javid, F. Sorrentino, T.R. Ioerger, J.C. Sacchettini, F. Manetti, M. Botta, A. De Logu, E.J. Rubin, E. De Rossi, MmpL3 is the cellular target of the antitubercular pyrrole derivative BM212, Antimicrob. Agents Chemother., 56 (2012) 324-331.

[17] S. Rao, S. Lakshminarayana, R. Kondreddi, M. Herve, L. Camacho, P. Bifani, S. Kalapala, J. Jiricek, N. Ma, B. Tan, S. Ng, M. Nanjundappa, S. Ravindran, P.G. Seah, P. Thayalan, S. Lim, B.H. Lee, A. Goh, W. Barnes, U. Manjunatha, Indolcarboxamide is a preclinical candidate for treating multidrug-resistant tuberculosis, Sci. Transl. Med., 5 (2013) 214ra168.

[18] V. Makarov, G. Manina, K. Mikusova, U. Möllmann, O. Ryabova, B. Saint-Joanis, N. Dhar, M.R. Pasca, S. Buroni, A.P. Lucarelli, A. Milano, E. De Rossi, M. Belanova, A. Bobovska, P. Dianiskova, J. Kordulakova, C. Sala, E. Fullam, P. Schneider, J.D. McKinney, P. Brodin, T. Christophe, S. Waddell, P. Butcher, J. Albrethsen, I. Rosenkrands, R. Brosch, V. Nandi, S. Bharath, S. Gaonkar, R.K. Shandil, V. Balasubramanian, T. Balganesh, S. Tyagi, J. Grosset, G. Riccardi, S.T. Cole, Benzothiazinones kill Mycobacterium tuberculosis by blocking arabinan synthesis, Science, 324 (2009) 801-804.

[19] R. Chikhale, S. Menghani, R. Babu, R. Bansode, G. Bhargavi, N. Karodia, M.V. Rajasekharan, A. Paradkar, P. Khedekar, Development of selective DprE1 inhibitors: Design, synthesis, crystal structure and antitubercular activity of benzothiazolylpyrimidine-5-carboxamides, Eur. J. Med. Chem., 96 (2015) 30-46.

[20] P.S. Shirude, R. Shandil, C. Sadler, M. Naik, V. Hosagrahara, S. Hameed, V. Shinde, C. Bathula, V. Humnabadkar, N. Kumar, J. Reddy, V. Panduga, S. Sharma, A. Ambady, N. Hegde, J. Whiteaker, R.E. McLaughlin, H. Gardner, P. Madhavapeddi, V. Ramachandran, P. Kaur, A. Narayan, S. Guptha, D. Awasthy, C. Narayan, J. Mahadevaswamy, K.G. Vishwas, V. Ahuja, A. Srivastava, K.R. Prabhakar, S. Bharath, R. Kale, M. Ramaiah, N.R. Choudhury, V.K. Sambandamurthy, S. Solapure, P.S. Iyer, S. Narayanan, M. Chatterji, Azaindoles: Noncovalent DprE1 inhibitors from scaffold morphing efforts, kill Mycobacterium tuberculosis and are efficacious in vivo, J. Med. Chem., 56 (2013) 9701-9708.

[21] M. Naik, V. Humnabadkar, S.J. Tantry, M. Panda, A. Narayan, S. Guptha, V. Panduga, P. Manjrekar, L.k. Jena, K. Koushik, G. Shanbhag, S. Jatheendranath, M.R. Manjunatha, G. Gorai, C. Bathula, S. Rudrapatna, V. Achar, S. Sharma, A. Ambady, N. Hegde, J. Mahadevaswamy, P. Kaur, V.K. Sambandamurthy, D. Awasthy, C. Narayan, S. Ravishankar, P. Madhavapeddi, J. Reddy, K.R. Prabhakar, R. Saralaya, M. Chatterji, J. Whiteaker, B. McLaughlin, L.R. Chiarelli, G. Riccardi, M.R. Pasca, C. Binda, J. Neres, N. Dhar, F. Signorino-Gelo, J.D. McKinney, V. Ramachandran, R. Shandil, R. Tommasi, P.S. Iyer, S. Narayanan, V. Hosagrahara, S. Kavanagh, N. Dinesh, S.R. Ghorpade, 4-Aminoquinolone piperidine amides: Noncovalent inhibitors of DprE1 with long residence time and potent antimycobacterial activity, J. Med. Chem., 57 (2014) 5419-5434.

[22] T.V. Sravanthi, S.L. Manju, Indoles — A promising scaffold for drug development, Eur. J. Pharm. Sci., 91 (2016) 1-10.

[23] M. Demurtas, A. Baldisserotto, I. Lampronti, D. Moi, G. Balboni, S. Pacifico, S. Vertuani, S. Manfredini, V. Onnis, Indole derivatives as multifunctional drugs: Synthesis and evaluation

of antioxidant, photoprotective and antiproliferative activity of indole hydrazones, Bioorg. Chem., 85 (2019) 568-576.

[24] A. Cutignano, G. Bifulco, I. Bruno, A. Casapullo, L. Gomez-Paloma, R. Riccio, Dragmacidin F: A new antiviral bromoindole alkaloid from the mediterranean sponge Halicortex sp, Tetrahedron, 56 (2000) 3743-3748.

[25] M.F. Abo-Ashour, W.M. Eldehna, R.F. George, M.M. Abdel-Aziz, M.M. Elaasser, N.M. Abdel Gawad, A. Gupta, S. Bhakta, S.M. Abou-Seri, Novel indole-thiazolidinone conjugates: Design, synthesis and whole-cell phenotypic evaluation as a novel class of antimicrobial agents, Eur. J. Med. Chem., 160 (2018) 49-60.

[26] L.J. Scott, C.M. Perry, Delavirdine:a review of its use in HIV infection, Drugs, 60 (2000) 1411-1444.

[27] G. Sanna, S. Madeddu, G. Giliberti, S. Piras, M. Struga, M. Wrzosek, G. Kubiak-Tomaszewska, A.E. Koziol, O. Savchenko, T. Lis, J. Stefanska, P. Tomaszewski, M. Skrzycki, D. Szulczyk, Synthesis and Biological Evaluation of Novel Indole-Derived Thioureas, Molecules, 23 (2018) 2554.

[28] K.P. Rakesh, H.K. Kumara, B.J. Ullas, J. Shivakumara, D. Channe Gowda, Amino acids conjugated quinazolinone-Schiff's bases as potential antimicrobial agents: Synthesis, SAR and molecular docking studies, Bioorg. Chem., 90 (2019) 103093.

[29] M. Scuotto, R. Abdelnabi, S. Collarile, C. Schiraldi, L. Delang, A. Massa, S. Ferla, A. Brancale, P. Leyssen, J. Neyts, R. Filosa, Discovery of novel multi-target indole-based derivatives as potent and selective inhibitors of chikungunya virus replication, Bioorg. Med. Chem., 25 (2017) 327-337.

[30] Â.C.F. Costa, S.C.H. Cavalcanti, A.S. Santana, A.P.S. Lima, T.B. Brito, R.R.B. Oliveira, N.A. Macêdo, P.F. Cristaldo, A.P.A. Araújo, L. Bacci, Insecticidal activity of indole derivatives against Plutella xylostella and selectivity to four non-target organisms, Ecotoxicology, 28 (2019) 973-982.

[31] A.S. Hogendorf, A. Hogendorf, K. Popiołek-Barczyk, A. Ciechanowska, J. Mika, G. Satała, M. Walczak, G. Latacz, J. Handzlik, K. Kieć-Kononowicz, E. Ponimaskin, S. Schade, A. Zeug, M. Bijata, M. Kubicki, R. Kurczab, T. Lenda, J. Staroń, R. Bugno, B. Duszyńska, B. Pilarski, A.J. Bojarski, Fluorinated indole-imidazole conjugates: Selective orally bioavailable 5-HT7 receptor low-basicity agonists, potential neuropathic painkillers, Eur. J. Med. Chem., 170 (2019) 261-275.

[32] M.A. Bhat, M.A. Al-Omar, M. Raish, M.A. Ansari, H.A. Abuelizz, A.H. Bakheit, A.M. Naglah, Indole derivatives as cyclooxygenase inhibitors: Synthesis, biological evaluation and docking studies, Molecules, 23 (2018) 1250.

[33] S.R. Bampi, A.M. Casaril, M. Domingues, D. de Andrade Lourenço, A.P. Pesarico, B. Vieira, K.R. Begnini, F.K. Seixas, T.V. Collares, E.J. Lenardão, L. Savegnago, Depression-like behavior, hyperglycemia, oxidative stress, and neuroinflammation presented in diabetic mice are reversed by the administration of 1-methyl-3-(phenylselanyl)-1H-indole, J. Psychiatr. Res., 120 (2020) 91-102.

[34] K.P. Rakesh, C.S. Shantharam, M.B. Sridhara, H.M. Manukumar, H.-L. Qin, Benzisoxazole: a privileged scaffold for medicinal chemistry, MedChemComm, 8 (2017) 2023-2039.

[35] M.N. Peerzada, P. Khan, K. Ahmad, M.I. Hassan, A. Azam, Synthesis, characterization and biological evaluation of tertiary sulfonamide derivatives of pyridyl-indole based heteroaryl chalcone as potential carbonic anhydrase IX inhibitors and anticancer agents, Eur. J. Med. Chem., 155 (2018) 13-23.

[36] W. Zhu, X. Bao, H. Ren, Y. Da, D. Wu, F. Li, Y. Yan, L. Wang, Z. Chen, N-Phenyl indole derivatives as AT1 antagonists with anti-hypertension activities: Design, synthesis and biological evaluation, Eur. J. Med. Chem., 115 (2016) 161-178.

[37] E. Vitaku, D.T. Smith, J.T. Njardarson, Analysis of the structural diversity, substitution patterns, and frequency of nitrogen heterocycles among U.S. FDA approved pharmaceuticals, J. Med. Chem., 57 (2014) 10257-10274.

[38] S.P.S. Rao, S.B. Lakshminarayana, R.R. Kondreddi, M. Herve, L.R. Camacho, P. Bifani, S.K. Kalapala, J. Jiricek, N.L. Ma, B.H. Tan, S.H. Ng, M. Nanjundappa, S. Ravindran, P.G. Seah, P. Thayalan, S.H. Lim, B.H. Lee, A. Goh, W.S. Barnes, Z. Chen, K. Gagaring, A.K. Chatterjee, K. Pethe, K. Kuhen, J. Walker, G. Feng, S. Babu, L. Zhang, F. Blasco, D. Beer, M. Weaver, V. Dartois, R. Glynne, T. Dick, P.W. Smith, T.T. Diagana, U.H. Manjunatha, Indolcarboxamide Is a Preclinical Candidate for Treating Multidrug-Resistant Tuberculosis, Sci. Transl. Med., 5 (2013) 214ra168.

[39] W. Li, A. Upadhyay, F.L. Fontes, E.J. North, Y. Wang, D.C. Crans, A.E. Grzegorzewicz, V. Jones, S.G. Franzblau, R.E. Lee, D.C. Crick, M. Jackson, Novel insights into the mechanism of inhibition of MmpL3, a target of multiple pharmacophores in Mycobacterium tuberculosis, Antimicrob. Agents Chemother., 58 (2014) 6413.

[40] C. Zhuang, W. Zhang, C. Sheng, W. Zhang, C. Xing, Z. Miao, Chalcone: A Privileged Structure in Medicinal Chemistry, Chem. Rev., 117 (2017) 7762-7810.

[41] Y. Cao, W. Xu, Y. Huang, X. Zeng, Licochalcone B, a chalcone derivative from Glycyrrhiza inflata, as a multifunctional agent for the treatment of Alzheimer's disease, Nat. Prod. Res, 34 (2018) 1-4.

[42] K. Baba, K. Nakata, M. Taniguchi, T. Kido, M. Kozawa, Chalcones from Angelica keiskei, Phytochemistry, 29 (1990) 3907-3910.

[43] C.C.B. de Castro, P.S. Costa, G.T. Laktin, P.H.D. de Carvalho, R.B. Geraldo, J. de Moraes, P.L.S. Pinto, M.R.C. Couri, P.d.F. Pinto, A.A. Da Silva Filho, Cardamonin, a schistosomicidal chalcone from Piper aduncum L. (Piperaceae) that inhibits Schistosoma mansoni ATP diphosphohydrolase, Phytomedicine, 22 (2015) 921-928.

[44] R.N. Gacche, N.A. Dhole, S.G. Kamble, B.P. Bandgar, In-vitro evaluation of selected chalcones for antioxidant activity, J. Enzyme Inhib. Med. Chem., 23 (2008) 28-31.

[45] Y.-M. Huang, N.S. Alharbi, B. Sun, C.S. Shantharam, K.P. Rakesh, H.-L. Qin, Synthetic routes and structure-activity relationships (SAR) of anti-HIV agents: A key review, Eur. J. Med. Chem., 181 (2019) 111566.

[46] M. Xu, Y. Peng, L. Zhu, S. Wang, J. Ji, K.P. Rakesh, Triazole derivatives as inhibitors of Alzheimer's disease: Current developments and structure-activity relationships, Eur. J. Med. Chem., 180 (2019) 656-672.

[47] X. Zhang, K.P. Rakesh, S.N.A. Bukhari, M. Balakrishna, H.M. Manukumar, H.-L. Qin, Multi-targetable chalcone analogs to treat deadly Alzheimer's disease: Current view and upcoming advice, Bioorg. Chem., 80 (2018) 86-93.

[48] C. Zhao, K.P. Rakesh, L. Ravidar, W.-Y. Fang, H.-L. Qin, Pharmaceutical and medicinal significance of sulfur (SVI)-Containing motifs for drug discovery: A critical review, Eur. J. Med. Chem., 162 (2019) 679-734.

[49] M. Xu, P. Wu, F. Shen, J. Ji, K.P. Rakesh, Chalcone derivatives and their antibacterial activities: Current development, Bioorg. Chem., 91 (2019) 103133.

[50] W.-Y. Fang, L. Ravindar, K.P. Rakesh, H.M. Manukumar, C.S. Shantharam, N.S. Alharbi, H.-L. Qin, Synthetic approaches and pharmaceutical applications of chloro-containing molecules for drug discovery: A critical review, Eur. J. Med. Chem., 173 (2019) 117-153.

[51] S. Park, E.H. Kim, J. Kim, S.H. Kim, I. Kim, Biological evaluation of indolizine-chalcone hybrids as new anticancer agents, Eur. J. Med. Chem., 144 (2018) 435-443.

[52] R.H. Hans, E.M. Guantai, C. Lategan, P.J. Smith, B. Wan, S.G. Franzblau, J. Gut, P.J. Rosenthal, K. Chibale, Synthesis, antimalarial and antitubercular activity of acetylenic chalcones, Bioorg. Med. Chem. Lett., 20 (2010) 942-944.

[53] H.-L. Qin, Z.-W. Zhang, R. Lekkala, H. Alsulami, K.P. Rakesh, Chalcone hybrids as privileged scaffolds in antimalarial drug discovery: A key review, Eur. J. Med. Chem., 193 (2020) 112215.

[54] P. Singh, A. Anand, V. Kumar, Recent developments in biological activities of chalcones: A mini review, Eur. J. Med. Chem., 85 (2014) 758-777.

[55] Y.S. El-Sayed, M. Gaber, Studies on chalcone derivatives: Complex formation, thermal behavior, stability constant and antioxidant activity, Spectrochim. Acta. A Mol. Biomol. Spectrosc., 137 (2015) 423-431.

[56] V.-J. Claudio, D. Amanda, B. Vanderlan da Silva, J.B. Eliezer, F. Carlos Alberto Manssour, Molecular Hybridization: A useful tool in the design of new drug prototypes, Curr. Med. Chem., 14 (2007) 1829-1852.

[57] G. Bérubé, An overview of molecular hybrids in drug discovery, EXPERT OPIN DRUG DIS, 11 (2016) 281-305.

[58] A. Özdemir, M.D. Altıntop, G. Turan-Zitouni, G.A. Çiftçi, İ. Ertorun, Ö. Alataş, Z.A. Kaplancıklı, Synthesis and evaluation of new indole-based chalcones as potential antiinflammatory agents, Eur. J. Med. Chem., 89 (2015) 304-309.

[59] S. Gupta, P. Maurya, A. Upadhyay, P. Kushwaha, S. Krishna, M.I. Siddiqi, K.V. Sashidhara, D. Banerjee, Synthesis and bio-evaluation of indole-chalcone based benzopyrans as promising antiligase and antiproliferative agents, Eur. J. Med. Chem., 143 (2018) 1981-1996.

[60] J. Yan, J. Chen, S. Zhang, J. Hu, L. Huang, X. Li, Synthesis, evaluation, and mechanism study of novel Indole-Chalcone derivatives exerting effective antitumor activity through microtubule destabilization in vitro and in vivo, J. Med. Chem., 59 (2016) 5264-5283.

[61] P. Makam, R. Kankanala, A. Prakash, T. Kannan, 2-(2-Hydrazinyl)thiazole derivatives: Design, synthesis and in vitro antimycobacterial studies, Eur. J. Med. Chem., 69 (2013) 564-576.

[62] P. Makam, T. Kannan, 2-Aminothiazole derivatives as antimycobacterial agents: Synthesis, characterization, in vitro and in silico studies, Eur. J. Med. Chem., 87 (2014) 643-656.

[63] O. Trott, A.J. Olson, AutoDock Vina: improving the speed and accuracy of docking with a new scoring function, efficient optimization, and multithreading, J. Comput. Chem., 31 (2010) 455-461.

[64] S. Dallakyan, A.J. Olson, Small-molecule library screening by docking with PyRx, in: J.E. Hempel, C.H. Williams, C.C. Hong (Eds.) Chemical Biology: Methods and Protocols, Springer New York, New York, NY, 2015, pp. 243-250.

[65] BIOVIA discovery studio visualizer in, Dassault Systemes Biovia Corp, 2019.

[66] C.A. Lipinski, F. Lombardo, B.W. Dominy, P.J. Feeney, Experimental and computational approaches to estimate solubility and permeability in drug discovery and development settings, Adv. Drug Deliv. Rev, 23 (1997) 3-25.

[67] D.F. Veber, S.R. Johnson, H.-Y. Cheng, B.R. Smith, K.W. Ward, K.D. Kopple, Molecular properties that influence the oral bioavailability of drug candidates, J. Med. Chem., 45 (2002) 2615-2623.

[68] Molinspiration Cheminformatics, https://www.molinspiration.com/cgi-bin/properties, in.

[69] A. Daina, O. Michielin, V. Zoete, SwissADME: a free web tool to evaluate pharmacokinetics, drug-likeness and medicinal chemistry friendliness of small molecules, Sci. Rep., 7 (2017) 42717.

[70] T.L.B. Douglas E. V. Pires, David B. Ascher, pkCSM: Predicting small-molecule pharmacokinetic and toxicity properties using graph-based signatures, J. Med. Chem., (2015).

[71] K.V. Sashidhara, R.P. Dodda, R. Sonkar, G.R. Palnati, G. Bhatia, Design and synthesis of novel indole-chalcone fibrates as lipid lowering agents, Eur. J. Med. Chem., 81 (2014) 499-509.

[72] M. Salfinger, L.B. Heifets, Determination of pyrazinamide MICs for Mycobacterium tuberculosis at different pHs by the radiometric method, Antimicrob. Agents Chemother., 32 (1988) 1002-1004.

[73] B. Zhang, J. Li, X. Yang, L. Wu, J. Zhang, Y. Yang, Y. Zhao, L. Zhang, X. Yang, X. Yang, X. Cheng, Z. Liu, B. Jiang, H. Jiang, L.W. Guddat, H. Yang, Z. Rao, Crystal Structures of Membrane Transporter MmpL3, an Anti-TB Drug Target, Cell, 176 (2019) 636-648.e613.

[74] J. Piton, S. Petrella, M. Delarue, G. Andre-Leroux, V. Jarlier, A. Aubry, C. Mayer, Structural insights into the quinolone resistance mechanism of Mycobacterium tuberculosis DNA gyrase, PLoS One, 5 (2010) e12245.

[75] P.S. Shirude, P. Madhavapeddi, J.A. Tucker, K. Murugan, V. Patil, H. Basavarajappa, A.V. Raichurkar, V. Humnabadkar, S. Hussein, S. Sharma, V.K. Ramya, C.B. Narayan, T.S. Balganesh, V.K. Sambandamurthy, Aminopyrazinamides: novel and specific GyrB inhibitors that kill replicating and nonreplicating Mycobacterium tuberculosis, ACS Chem. Biol., 8 (2013) 519-523.

[76] D.A. Rozwarski, G.A. Grant, D.H. Barton, W.R. Jacobs, Jr., J.C. Sacchettini, Modification of the NADH of the isoniazid target (InhA) from Mycobacterium tuberculosis, Science, 279 (1998) 98-102.

[77] S.M. Batt, T. Jabeen, V. Bhowruth, L. Quill, P.A. Lund, L. Eggeling, L.J. Alderwick, K. Futterer, G.S. Besra, Structural basis of inhibition of Mycobacterium tuberculosis DprE1 by benzothiazinone inhibitors, Proc. Natl. Acad. Sci. U. S. A., 109 (2012) 11354-11359.

[78] D. Leys, C.G. Mowat, K.J. McLean, A. Richmond, S.K. Chapman, M.D. Walkinshaw, A.W. Munro, Atomic structure of Mycobacterium tuberculosis CYP121 to 1.06 A reveals novel features of cytochrome P450, J. Biol. Chem., 278 (2003) 5141-5147.

[79] S.R. Luckner, C.A. Machutta, P.J. Tonge, C. Kisker, Crystal structures of Mycobacterium tuberculosis KasA show mode of action within cell wall biosynthesis and its inhibition by thiolactomycin, Structure, 17 (2009) 1004-1013.

[80] S.R. Luckner, C.A. Machutta, P.J. Tonge, C. Kisker, Crystal structures of Mycobacterium tuberculosis KasA show mode of action within cell wall biosynthesis and its inhibition by thiolactomycin, Structure, 17 (2009) 1004-1013.

[81] C. Ratledge, Iron, mycobacteria and tuberculosis, Tuberculosis, 84 (2004) 110-130.

[82] L. Cronje, L. Bornman, Iron overload and tuberculosis: a case for iron chelation therapy, IJTLD, 9 (2005) 2-9.

[83] D.K. Mahapatra, S.K. Bharti, V. Asati, S.K. Singh, Perspectives of medicinally privileged chalcone based metal coordination compounds for biomedical applications, Eur. J. Med. Chem., 174 (2019) 142-158.

[84] J. Johnson, A. Yardily, Chalconoid metal chelates: spectral, biological and catalytic applications, J. Coord. Chem., 72 (2019) 2437-2488.

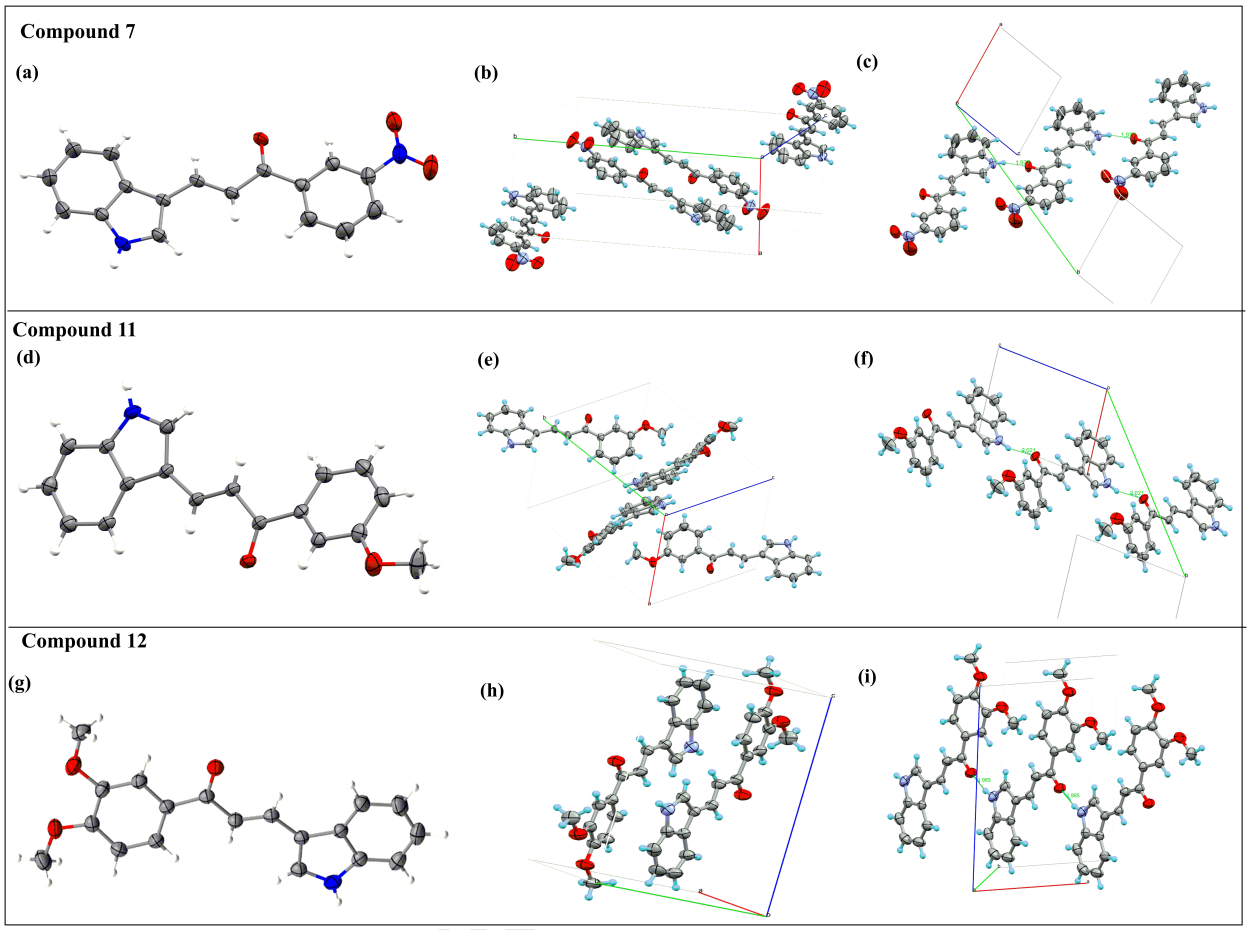

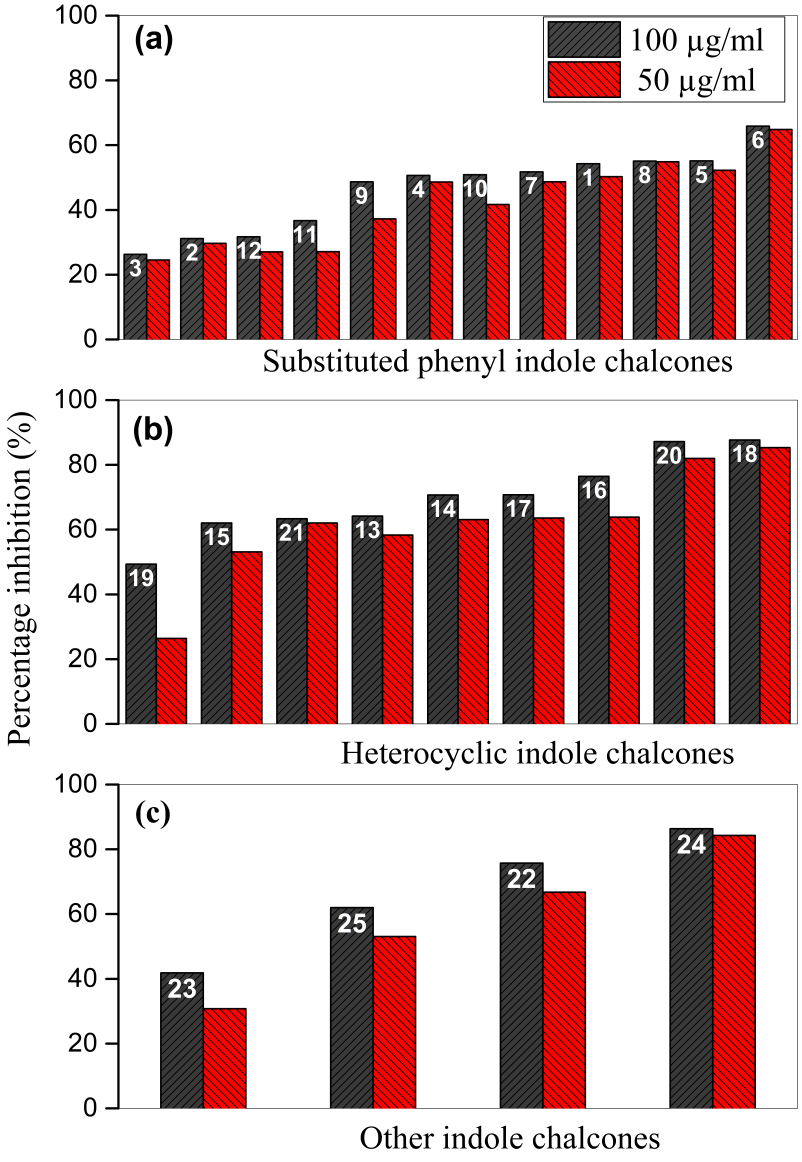
(a)
100 µg/ml
50 µg/ml
3
2
12
11
9
4
10
7
1
8
5
6
Substituted phenyl indole chalcones
(b)
19
15
21
13
14
17
16
20
18
Heterocyclic indole chalcones
(c)
23
25
22
24
Other indole chalcones
Percentage inhibition (%)
0
20
40
60
80
100

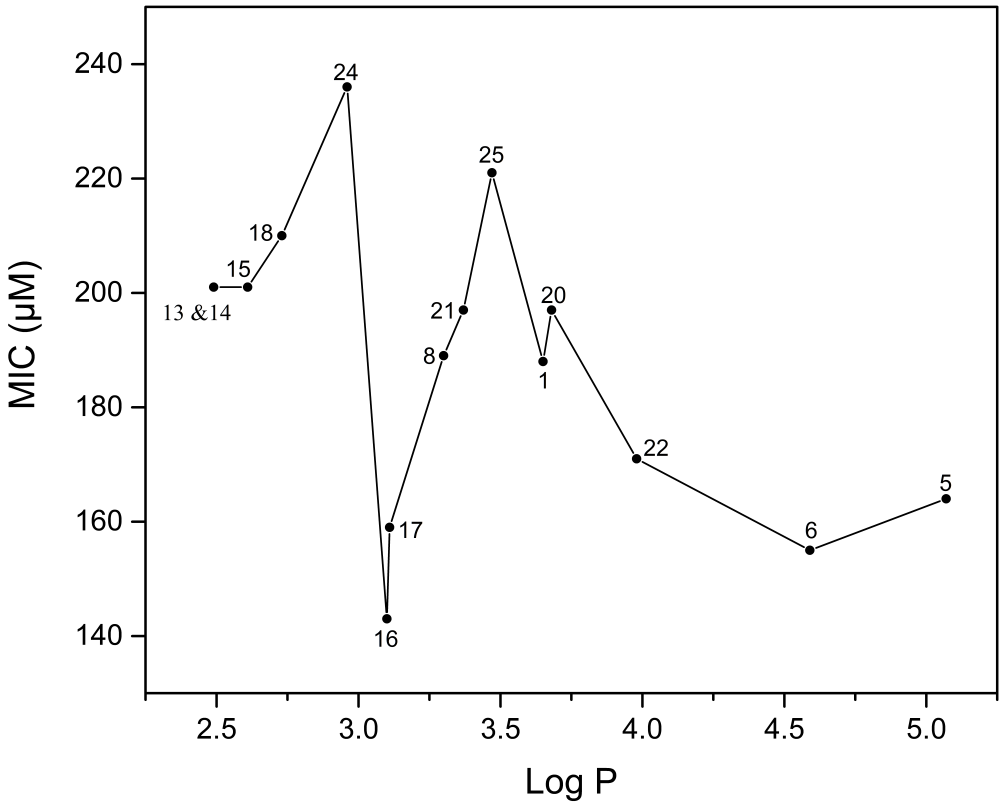
MIC (μM)
240
220
200
180
160
140
24
25
18
15
13 &14
21
20
8
1
22
5
17
6
16
2.5
3.0
3.5
4.0
4.5
5.0
Log P

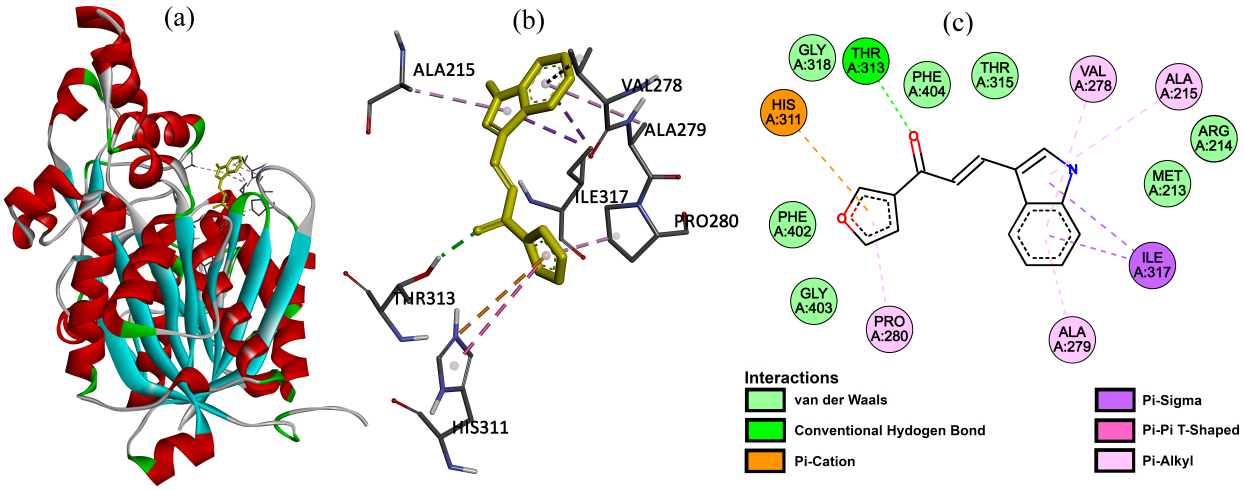

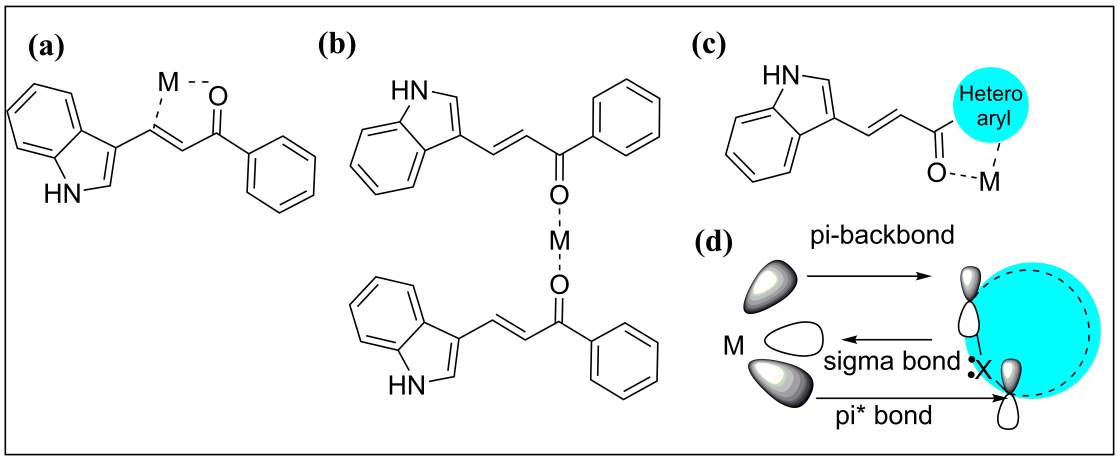

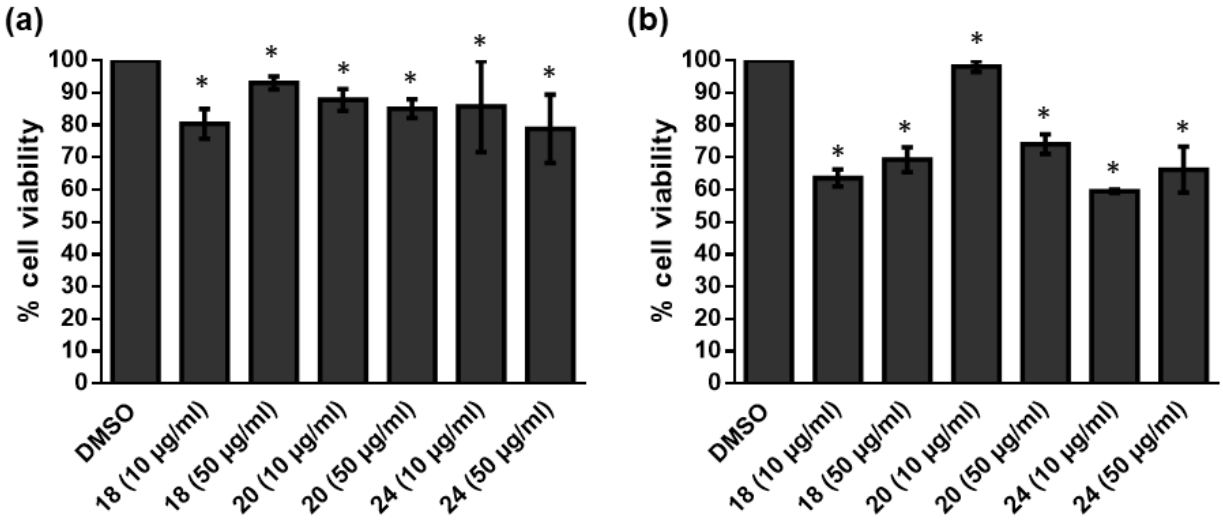

(a)

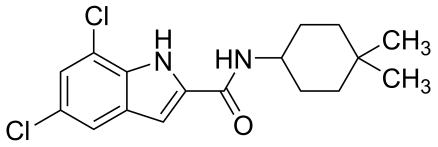

NITD-304

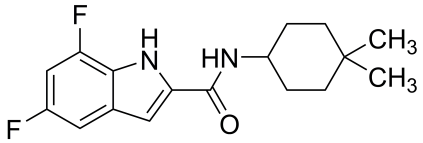

NITD-349

(b)

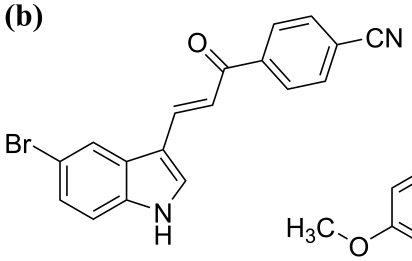

Anti-inflammatory agent

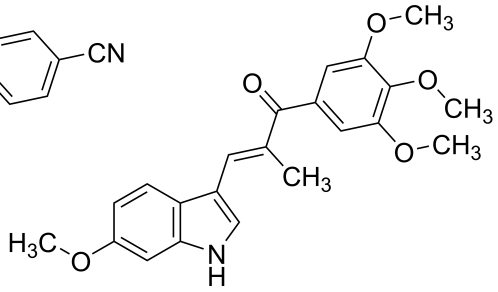

Anticancer agent

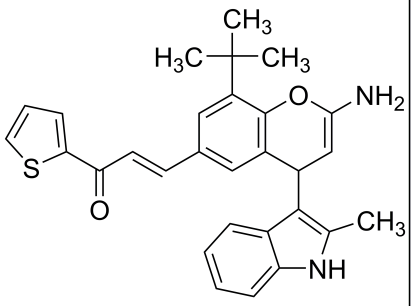

Antiproliferative agent

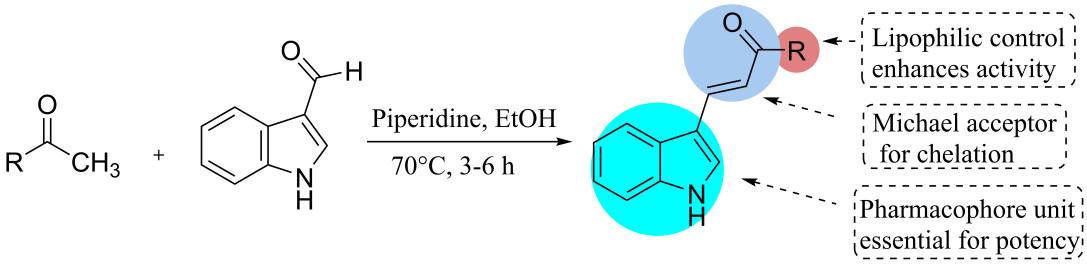

1. R= 4-F-C_6H_5
2. R= 4-CF_3-C_6H_5
3. R= 3-CF_3-C_6H_5
4. R= 4-Cl-C_6H_5
5. R= 2,4-Cl-C_6H_5
6. R= 4-Br-C_6H_5
7. R= 3-NO_2-C_6H_5
8. R= 4-HO-C_6H_5
9. R= 3-NH_2-C_6H_5
10. R= 4-CH_3-C_6H_5
11. R= 3-OCH_3-C_6H_5
12. R= 3,4-OCH_3-C_6H_5
13. R= 4-Pyridyl
14. R= 3-Pyridyl
15. R= 2-Pyridyl
16. R= 4-OH-4-C_6H_5-piperazine
17. R= 1-C_6H_5-imidazole
18. R= 3-furyl
19. R= 2-pyroyl
20. R= 2- thiophenyl
21. R= 3-thiophenyl
22. R= 1,3- benzodioxole
23. R= 2-naphthyl
24. R= cyclopentyl
25. R= cyclohexyl

Highlights

- Indole chalcones having DLM properties were designed and synthesized.
- Out of 25 indole chalcones, 15 compounds with heterocyclic moieties showed inhibition against H_{37}Rv strain of *MTb* with MIC value in the range of 143 and 236 µM.
- Three best compounds, 3-furyl, 2-thiophenyl, cyclopentyl substituted indole chalcones were non cytotoxic against Mo7e and BA/F3 cells.
- *In-silico* analysis against KasA protein was studied to understand plausible mode of antitubercular activity.

Declaration of interests

☒ The authors declare that they have no known competing financial interests or personal relationships that could have appeared to influence the work reported in this paper.

☐The authors declare the following financial interests/personal relationships which may be considered as potential competing interests: